TECTONICS, VOL. 12, NO. 3, PAGES 611-628, JUNE 1993

THERMOCHRONOLOGIC CONSTRAINTS ON THE TECTONIC EVOLUTION OF ACTIVE METAMORPHIC CORE COMPLEXES, D'ENTRECASTEAUX ISLANDS, PAPUA NEW GUINEA

Suzanne L. Baldwin,[1,2] Gordon S. Lister,[3] E. June Hill,[3,4] David A. Foster,[5] and Ian McDougall[1]

Abstract. Metamorphic core complexes in the D'Entrecasteaux Islands, Papua New Guinea, formed as the result of active extension at the western end of the propagating Woodlark Basin spreading center. Domes of high-grade metamorphic rocks (i.e., amphibolites, eclogites, and migmatites), intruded by large granodiorite bodies, comprise the lower plate of the D'Entrecasteaux metamorphic core complexes. The domes are transected by kilometer-scale shear zones. A thermochronologic study of the D'Entrecasteaux Islands utilizing K/Ar, $^{40}Ar/^{39}Ar$, and fission track techniques has documented the unroofing history of these active metamorphic core complexes. Gneisses in the cores of the domes cooled rapidly (≥100°C/m.y.) as indicated by hornblende and biotite $^{40}Ar/^{39}Ar$ apparent ages of ~2.7 to 3.0 Ma and ~1.6 to 1.7 Ma, respectively, and apatite fission track ages of ~0.4 to 0.9 Ma. $^{40}Ar/^{39}Ar$ apparent ages on white mica, biotite, and potassium feldspar and fission track ages on apatites from shear zone gneisses indicate extremely rapid cooling (in some cases >500°C/m.y.) and suggest shear zones were active from 4.0 to 3.5 Ma and 1.9 to 1.4 Ma. In general, $^{40}Ar/^{39}Ar$ mineral ages for retrogressed core zone gneisses, shear zone gneisses, and granodiorites are 2.0 to 3.0 Ma (amphiboles), 1.5 to 1.7 Ma (muscovites), and 1.4 to 1.8 Ma (biotites) and 1.0 to 2.0 Ma (K-feldspars). Apatite fission track ages from core zone gneisses, shear zone gneisses and granodiorites range from 0.4 to 1.0 Ma. Thermochronologic results indicate that emplacement of granodiorites closely coincided with retrogression of the metamorphic basement and movement on the outer shear zones bounding the gneiss domes. The granodiorite bodies associated with the D'Entrecasteaux Islands domes represent syn-kinematically emplaced granitoids intruded into an area of active continental extension.

INTRODUCTION

Metamorphic core complexes were first recognized in the North American Cordillera [Crittenden et al., 1980, and references therein] and initially they appeared to represent tectonic features peculiar to the North American Cordillera. However, they are now recognized in many tectonic environments [Lister et al., 1984; Hill, 1987; Gibson, 1990], and examples of metamorphic core complexes potentially exist worldwide and throughout Earth's history. Metamorphic core complexes form as the result of major continental extension, when the middle and lower crust are dragged out beneath the fracturing, extending upper crust. In general, they are characterized by the following.

1. A lower plate which contains strongly deformed metamorphic and plutonic rocks. The lower plate typically has a domal or anticlinal geomorphology and it thus forms local topographic highs. The domes have been exposed as the result of erosional and tectonic denudation of the deformed crystalline metamorphic and igneous rocks. The lower plate rocks have been uplifted and exposed during continental extension.
2. An upper plate which contains tectonically detached and distended cover rocks. The upper plate contains rocks that were already at relatively shallow crustal levels prior to the onset of extension and is cut by numerous high-angle faults, listric normal faults, and low-angle faults.
3. A low-angle normal fault which separates rocks of the upper and lower plates. The fault cuts ductile shear zones on at least one side of the dome.

In recent years a considerable amount of research effort has focused on attempts to understand and quantify the mechanisms by which continental crust undergoes extension [Wernicke, 1981, 1985; Miller et al., 1983; Davis et al., 1986; Rehrig, 1986; Gans, 1987; Lister and Davis, 1989, and many others]. Studies which have focused on quantifying the timing of metamorphic and plutonic events and uplift histories of metamorphic core complexes have contributed much to our understanding of the unique combination of features and events that result in the very rapid localized extension in these terranes. The most successful of these studies have integrated data from several thermochronometric systems (e.g., $^{40}Ar/^{39}Ar$, fission track) to constrain the upward and lateral movements of core complexes through the middle and upper crust. The combination of isotopic closure temperature concepts with knowledge obtained from $^{40}Ar/^{39}Ar$ step heating experiments and fission track analyses has provided a powerful approach to the study of kinetic processes in these extensional terranes. The rapid cooling rates (>>40°C/m.y.) of the lower plates from temperatures above 400°C to below 60°C is now well documented for many metamorphic core complexes in western North America [Dokka and Lingrey, 1979; DeWitt et al., 1986; Dokka et al., 1986; Foster et al., 1990; Richard et al., 1990; Bryant et al., 1991; Carl et al., 1991]. Several integrated thermochronologic and structural studies have also been able to constrain the initial dips of detachment faults and estimate rates of extension during formation of core complexes [Foster et al., 1990; Richard et al., 1990; Gans et al., 1991].

In the Papua New Guinea region the transition from rifted to active continental margin is well displayed making this area ideal for studying active tectonic processes associated with continental extension [Audley-Charles, 1991]. Metamorphic core complexes in the D'Entrecasteaux Islands, Papua New Guinea [Hill, 1987, 1990; Davies and Warren, 1988] formed as the result of active extension at the western end of the propagating Woodlark Basin spreading center (Figure 1). The area provides a relatively unambiguous active tectonic setting in which to study extension of continental crust previously thickened during collisional orogenesis. In contrast with many older

[1]Research School of Earth Sciences, Australian National University, Canberra, Australian Capital Territory.
[2]Now at Department of Geosciences, University of Arizona, Tucson.
[3]Victorian Institute of Earth and Planetary Sciences Department of Earth Sciences, Monash University, Clayton, Victoria, Australia.
[4]Now at Department of Geology, University of Otago, Dunedin, New Zealand.
[5]Victorian Institute of Earth and Planetary Sciences Department of Geology, La Trobe University, Bundoora, Victoria, Australia.

Paper number 93TC00235.
0278-7407/93/93TC-00235$10.00

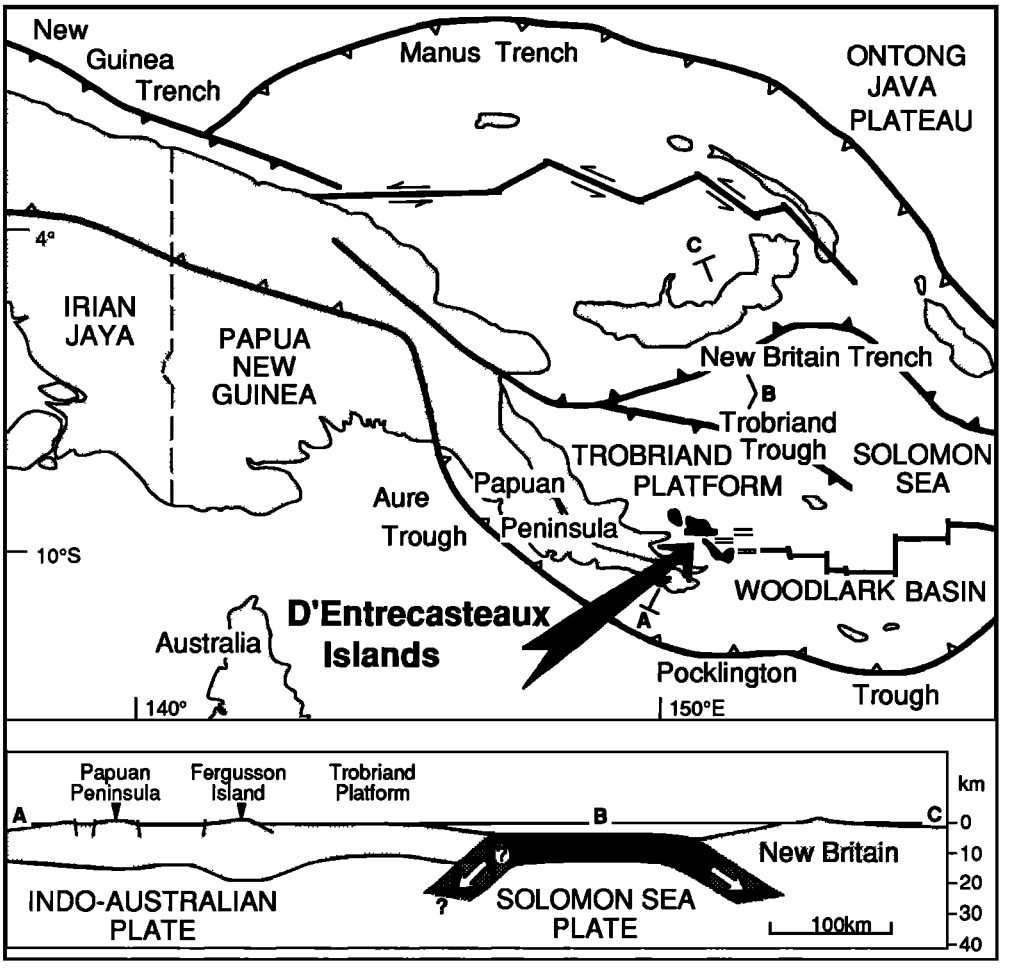

Fig. 1. Regional tectonic setting of the D'Entrecasteaux Islands, southeastern Papua New Guinea [after Cooper and Taylor, 1987].

orogenic belts, the features associated with the evolution of this active metamorphic core complex are relatively unobscured because the area has undergone no overprinting by later tectonic or thermal events since their formation in Plio-Pleistocene time. Regional tectonics, geomorphology and seismic activity [Abers, 1991] indicate that the core complexes may still be actively forming.

This paper presents results of K/Ar, $^{40}Ar/^{39}Ar$, and fission track studies of the metamorphic basement, shear zones, and intrusions of the D'Entrecasteaux Islands aimed at documenting the unroofing and cooling history of the youngest reported metamorphic core complex on Earth. Results have provided insight into the role of igneous processes in the uplift and development of domes, as well as the thermal consequences of ridge propagation into previously thickened continental crust.

TECTONIC SETTING

The tectonics of the Papua New Guinea (PNG) region are the result of interactions between microplates caught in and formed during the large-scale collision of the Pacific plate and the Indo-Australian plate (Figure 1) [Johnson and Molnar, 1972; Curtis, 1973; Cooper and Taylor, 1987]. Geochemical and geophysical data suggest a long history of subduction-related processes in this area [Johnson et al., 1978; Weissel et al., 1982; Cooper and Taylor, 1987]. At present, rates of plate tectonic motion are high in this region (e.g., 13 cm/yr across the New Britain trench [Stoltz et al., 1990]).

The most significant collisional event in the Papuan Peninsular region was the obduction of the Papuan Ultramafic Belt which occurred in late Eocene time [Davies and Smith, 1971]. Gravity data indicate the crust beneath the Papuan Peninsula is approximately 32 km thick, beneath the Trobriand Platform the crust is ~24 km thick, and the crust thins towards the Solomon Sea [Milsom and Smith, 1975]. A gravity trough, interpreted to be partly due to low-density intrusives and partly due to isostatic thickening, extends beneath the D'Entrecasteaux Islands with minima centered in northeastern Goodenough Island, western Fergusson Island, and the northern part of Normanby Island (Figure 2) [Milsom, 1973].

Westward propagation of seafloor spreading in the Woodlark Basin is accompanied by active continental extension in the D'Entrecasteaux Islands and flanking basins. The D'Entrecasteaux Islands lie on the western edge of the westerly propagating Woodlark Basin seafloor spreading system and mark an area where a spreading center intersects previously

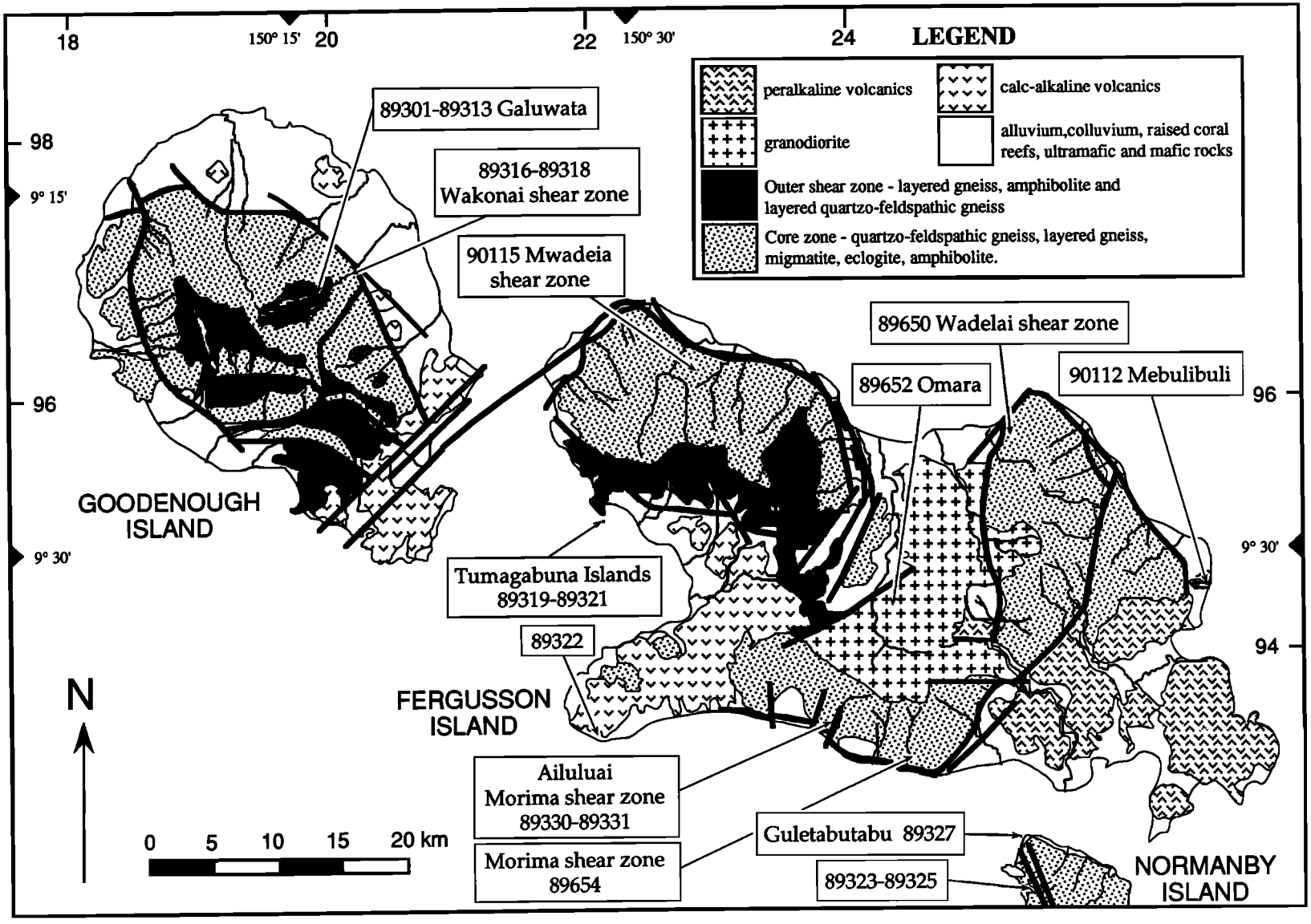

Fig. 2. Geologic map of the D'Entrecasteaux Islands after Davies and Ives [1965] and Hill [1991] showing location of samples used in this study.

thickened continental crust of the Papuan Peninsula. Davies et al. [1984] suggest that the basement gneisses of D'Entrecasteaux Islands are likely an extension of mainland sialic crust. The region is believed to have been extending since the Pliocene following an Oligocene collisional event which produced the Owen-Stanley Metamorphic belt. The line of domes continues onto the Papuan Peninsula where blueschists and low-grade metamorphic rocks are exposed in the Dayman dome [Worthing, 1988].

Magnetic anomaly data indicate sea floor spreading may have begun in the Woodlark Basin ~20 Ma (early Miocene [Luyendyk et al., 1973]). However, the main rifting phase did not begin until ~3.5 Ma [Weissel et al., 1982]. This magnetic data indicate the ridge trends WNW and is offset by several transform faults. There are two zones of spreading; a failed sediment-covered southern arm and an active northern arm which is propagating between Fergusson Island and Normanby Island [Binns et al., 1986]. Shallow normal fault plane solutions typify the D'Entrecasteaux Islands and southeastern Papua New Guinea; the events indicate the prevailing extension direction in the D'Entrecasteaux Islands region is ~NNE-SSW [Ripper, 1982]. The D'Entrecasteaux Islands are separated from the Papuan Peninsula by Goodenough Bay and Milne Bay which are WNW trending grabens or half graben. Active tectonism in the D'Entrecasteaux Islands region is indicated by raised coral reef terraces, active hydrothermal systems [Davies and Ives, 1965] and modern rift volcanism [Smith, 1976; Smith and Milsom, 1984].

GEOLOGY OF THE D'ENTRECASTEAUX ISLANDS

The D'Entrecasteaux Islands were first mapped and studied by Davies and Ives [1965] and subsequently by Davies [1973] and Davies and Warren [1988]. Studies of the geologic evolution of the islands also include those by Ollier and Pain [1980] and P. H. Masson (Structure of Fergusson Island, D'Entrecasteaux group, Papua New Guinea, report for Exxon Minerals Company, Houston, Texas, June 2, 1984). The D'Entrecasteaux Islands consist of three large islands, Goodenough Island, Fergusson Island,and Normanby Island and several smaller islands (Figure 2). The metamorphic core complexes of the D'Entrecasteaux Islands consist of multiply deformed and metamorphosed basement overlain by a cover of ultramafic rocks [Hill, 1991]. The ultramafic cover and metamorphic basement are separated by faults and are unconformably overlain by recent sediments and volcanic rocks. Four lithologic groups can be distinguished on the islands: a complexly deformed metamorphic basement which forms mountainous domes, largely undeformed mafic and ultramafic cover rocks, volcanic rocks, and intrusive rocks.

The metamorphic basement which forms mountainous domes can be divided into two structural zones: a core zone (i.e., "lower plate") and an outer sheared zone [Hill, 1990; Hill et al., 1992]. The core zone consists of eclogites, migmatites, gneissic and mylonitic rocks. Hill and Baldwin [1993] obtained peak metamorphic conditions of 18 to 21 kbar and 730° to 900°C for eclogitic rocks in the core zone. Davies and Warren [1993] have classified the eclogitic rocks into three types which indicate temperatures and pressure of equilibration ranging from 530° to 840°C and pressures of 12 to 24 kbar. Additional work on previously described mafic granulite facies rocks [Davies and Warren, 1988] from the metamorphic basement indicates they are Na-poor eclogites [Davies and Warren, 1993]. Subsequent retrogression of the core zone gneiss to amphibolite facies occurred at pressures of 7 to 11 kbar and temperatures of 570° to 730°C [Hill and Baldwin, 1993]. Greenschist facies rocks are restricted to areas that have experienced the very last stages of shear zone activity [Hill, 1991]. Structural fabrics in the core zone are highly variable and are the result of two deformation events [Hill et al., 1992]. The first deformation (D_1) resulted in gneissic layering that predates peak metamorphism. The second generation of deformation (D_2) postdates peak metamorphism and resulted in folding and boudinage of the gneissic layering and formation of retrograde foliations. Major and trace element concentrations of felsic gneisses, granodiorite, and eclogites indicates they were derived from predominantly igneous protoliths [Norman and Baldwin, 1990]. The whole rock chemistry of eclogites are comparable to average midocean ridge basalts compositions and to basalts of the Papuan Ultramafic Belt [Davies and Warren, 1993].

Curved kilometer scale shear zones and faults dipping outwards at angles of between 0 and 45 degrees form the outer sheared zone which envelops the core zone [Hill, 1990, 1991]. The shear zones contain rocks similar to those found in the core zone (i.e., layered mylonitic gneisses) although they have been sheared and retrogressed to lower amphibolite facies. Shear zone gneisses equilibrated at temperatures of 720° to 730°C and pressures of 10 to 11 kbar [Hill and Baldwin, 1993]. The evolution of the shear zones is characterized by progressive localization of structures, progressive retrograde metamorphism and a change from predominantly ductile to predominantly brittle deformation [Hill et al., 1992].

The "upper plate" is poorly exposed in the D'Entrecasteaux Islands region and consists primarily of recent volcanic rocks and serpentinized ultramafic rocks. The ultramafic rocks consist of altered dunite, harzburgite and pyroxenite. They are believed to be part of the Papuan Ultramafic Belt exposed on the mainland of Papua New Guinea and likely represent segments of oceanic crust which were thrust over sialic crust as a result of an Oligocene arc-continent collision [Davies and Ives, 1965; Davies and Jacques, 1984]. Most of the upper plate rocks are below sea level, so the relationship between the upper plate rocks and the metamorphic-plutonic basement is not known in detail.

Tertiary-Quaternary calc-alkaline and peralkaline volcanic rocks [Smith, 1976] overlie the ultramafic cover and basement. Calc-alkaline volcanic rocks range in age from 6 to 0.8 Ma [Smith and Compston, 1982; Smith and Milsom, 1984] (Table 1) and are believed to have been derived from a subduction modified mantle. Peralkaline rhyolites (comendites) on southeastern Fergusson Island are believed to be rift related. Volcanic centers are associated with faults and are still active [Smith, 1976].

The metamorphic basement and ultramafic rocks are intruded by granodiorite bodies and minor gabbro and dolerite dikes. Field evidence indicates felsic bodies and mafic dikes intruded the gneisses before, during and after the formation of the outer shear zone [Hill, 1991]. The size of the outcrop of granodiorite varies considerably. The best exposed pluton is the Omara granodiorite which lies in a relatively low topographic area between two of the basement domes on Fergusson Island and covers an area of approximately 150 km^2.

Previously reported K-Ar ages for biotites and muscovite for

TABLE 1. K/Ar Data and Apparent Ages of Feldspars and Whole Rock Samples from the D'Entrecasteaux Islands, PNG

Sample[a]	Rock Type	[K][b], wt %	$^{40}Ar^*$ x 10^{-11} mol g^{-1}	$\%^{40}Ar^*$	Age, Ma ± 1 s.d.
89301 (p)	felsic gneiss	1.01 1.04	1.66	11.5	9.29 ± 0.27
89309 (K)	granodiorite	10.81 10.81	3.65	42.1	1.95 ± 0.03
89323 (K)	quartzo-feldspathic schist	10.38 10.39	3.60	60.7	2.00 ± 0.02
89325 (K)	granodiorite	10.80 10.79	3.77	66.2	2.01 ± 0.02
89327 (K)	granodiorite	10.06 10.10	3.34	41.1	1.91 ± 0.02
89329 (K)	granodiorite	6.25 6.35	1.95	6.3	1.78 ± 0.07
89331 (K)	felsic gneiss	10.48 10.45	3.50	51.6	1.93 ± 0.02
89322 (wr)	andesite	3.94 3.97	0.55	11.0	0.79 ± 0.02
89324 (wr)	dolerite	2.12 2.11	0.65	13.4	1.78 ± 0.03

$\lambda_e + \lambda_e' = 0.581 \times 10^{-10}$ yr^{-1}, $\lambda_\beta = 4.962 \times 10^{-10}$ yr^{-1}; $^{40}K/K = 1.167 \times 10^{-4}$ mol mol^{-1}; $^{40}Ar^*$ = radiogenic argon.

[a]Material analyzed indicated in parentheses; plagioclase (p), K-feldspar (K), whole rock (wr).

[b]Duplicate analyses.

leucogneiss and granodiorites from the D'Entrecasteaux Islands range from 1.9 to 3.7 Ma and have been interpreted to represent the time of cooling after granodiorite intrusion and uplift [Davies, 1973; Davies and Warren, 1988].

ANALYTICAL TECHNIQUES

K/Ar, $^{40}Ar/^{39}Ar$, and fission track analyses were used to obtain thermochronologic data for the core zone gneisses, the shear zone gneisses, and intrusives. High-purity mineral separates (>99% pure) were prepared from crushed and sized rock chips using conventional heavy liquid and magnetic separation techniques.

For K-Ar analyses, the potassium concentration was measured on a split of the sample using flame photometry with a sodium sulfate buffer and a lithium internal standard. The argon concentration was determined by isotope dilution in a mass spectrometer using a high-purity ^{38}Ar tracer. K-Ar procedures followed those described by McDougall [1985]. K-Ar results are shown in Table 1. The error in K-Ar age is determined by quadratically combining uncertainties associated with measurement of the potassium concentration, radiogenic ^{40}Ar and ^{38}Ar in the spike. Ages quoted are calculated assuming that nonradiogenic Ar in the sample is of atmospheric composition.

For $^{40}Ar/^{39}Ar$ analyses mineral separates were irradiated for 80 hours in position X34, or X33 of the HIFAR nuclear reactor of the Australian Nuclear Science and Technology Organization at Lucas Heights, New South Wales. Irradiation procedures followed those described by McDougall and Harrison [1988]. Biotite standard GA1550 (97.9 Ma [McDougall and Roksandic, 1974]) and hornblende standard 77600 (414.1 Ma [Harrison, 1981]) were used to monitor the neutron dose. $^{40}Ar/^{39}Ar$ procedures followed those described by McDougall [1985]. For age calculation, the data have been corrected for machine mass discrimination, decay of ^{37}Ar and ^{39}Ar and for neutron-induced interfering isotopes [Tetley et al., 1980]. Correction factors used to account for interfering nuclear reactions are listed in Table 2[1] and were determined by analyzing argon extracted from irradiated CaF_2 and K_2SO_4. Machine discrimination was determined from repeated analysis of atmospheric argon, and line blanks were measured at different temperatures prior to analyses. Results of $^{40}Ar/^{39}Ar$ step heat and total fusion experiments are shown in Table 2 and age spectra are shown in Figures 3-5. All ages are calculated using the decay constants recommended by Steiger and Jager [1977]. Stated precisions for $^{40}Ar/^{39}Ar$ ages include all uncertainties in the measurement of isotope ratios and are quoted at the 1σ level. The errors do not include an error associated with the J parameter which is < 0.5%.

For fission track analyses analytical procedures followed the techniques described by Green [1986]. Apatites were mounted

[1]Table 2 is available with entire article on microfiche. Order from American Geophysical Union, 2000 Florida Avenue, N.W., Washington, DC 20009. Document T93-001; $2.50 payment must accompany order.

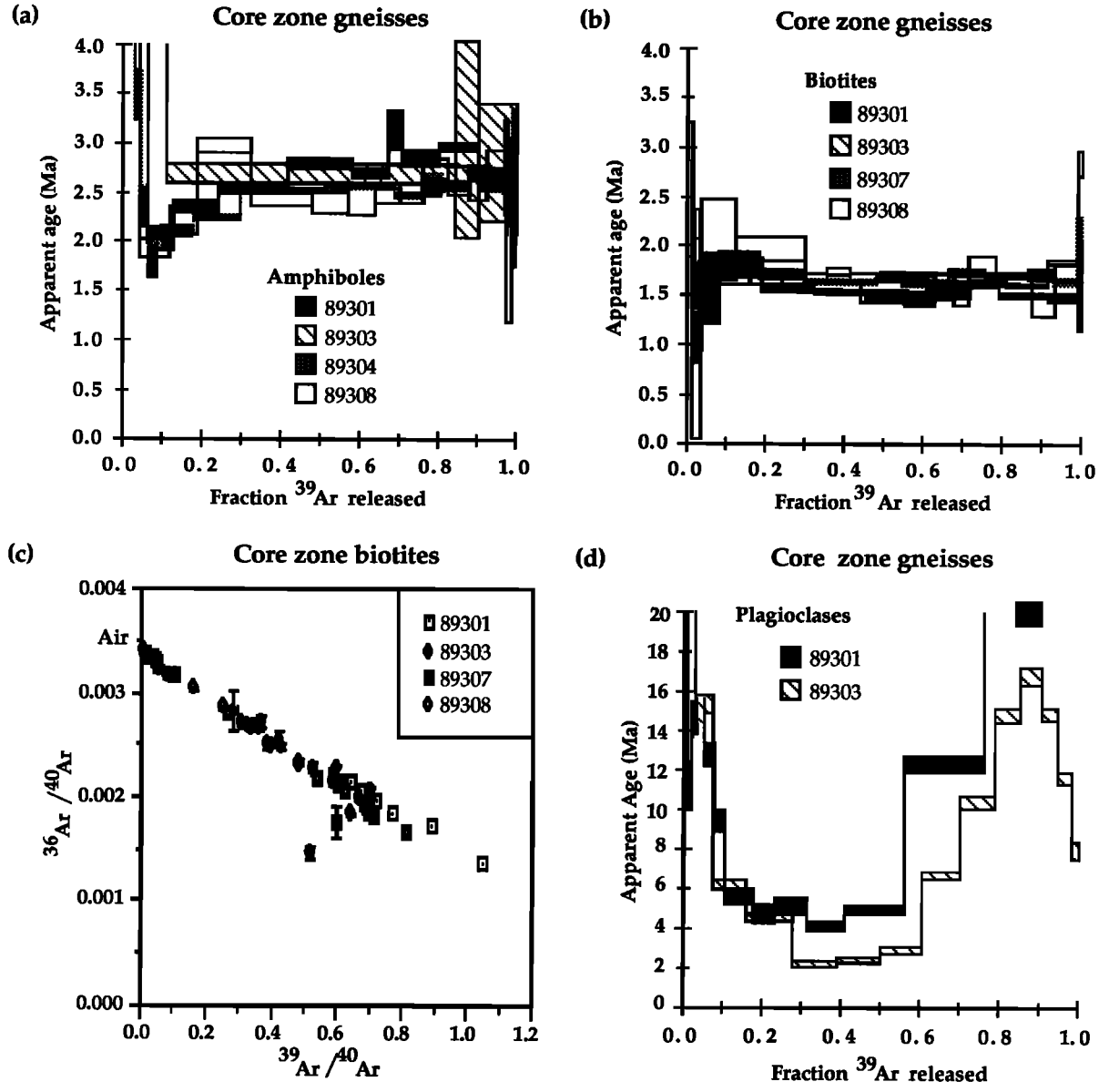

Fig. 3. (a) $^{40}Ar/^{39}Ar$ age spectra for amphiboles from core zone gneisses, Goodenough Island; (b) $^{40}Ar/^{39}Ar$ age spectra for biotites from core zone gneisses, Goodenough Island; (c) inverse isochron plot for core zone biotites; (d) $^{40}Ar/^{39}Ar$ age spectra for plagioclases from core zone gneisses, Goodenough Island.

in epoxy resin on glass slides, ground and polished to reveal an internal surface, and then etched in 5N HNO_3 at room temperature to reveal fossil fission tracks. Samples were irradiated in the X-7 position of the HIFAR nuclear reactor of the Australian Nuclear Science and Technology Organization. Thermal neutron fluences were monitored in a muscovite detector adjacent to discs of NBS standard glass SRM612. Ages were determined by the external detector method with a low-uranium muscovite used to record induced tracks during irradiation. Fission tracks in apatites were counted at magnifications of 1250x using a dry objective; only those grains oriented parallel to the c axis that displayed sharp polishing scratches were counted. Ages were calculated using the zeta calibration method of Hurford and Green [1982] and Green [1985]. Uncertainties in fission track ages were calculated using standard statistical methods [Green, 1981] and are reported at the 1σ level. Results of fission track analyses are shown in Table 3. A summary of all the thermochronologic data for samples from the D'Entrecasteaux Islands is shown in Table 4.

RESULTS

Core Zone Rocks

$^{40}Ar/^{39}Ar$ and K/Ar results. The quartzo-feldspathic gneisses studied contain a primary assemblage of plagioclase +

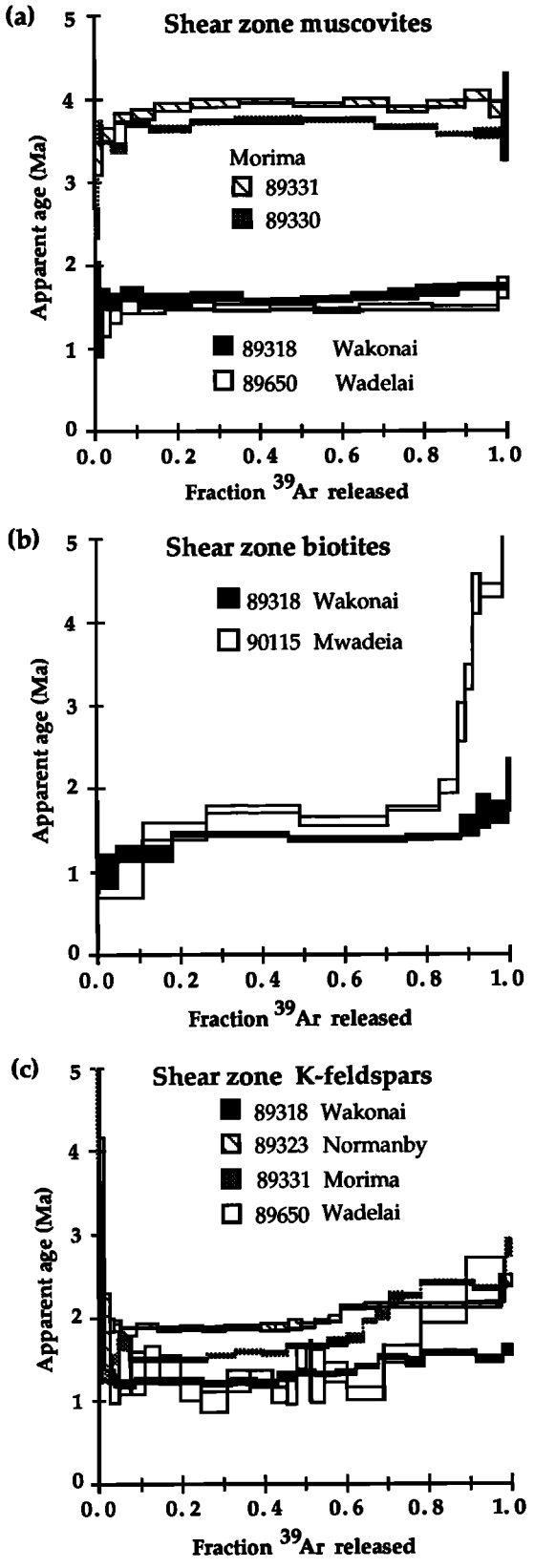

Fig. 4. $^{40}Ar/^{39}Ar$ age spectra for (a) muscovites, (b) biotites, and (c) K-feldspars from the D'Entrecasteaux Island shear zones.

quartz + garnet + rutile ± pyroxene ± amphibole. Retrograde assemblages include biotite and hornblende coronas around garnet, amphibole replacing pyroxene and minor sericitization of plagioclase. Eclogites contain a primary assemblage of almandine-pyrope + omphacite ± quartz ± rutile with a retrograde assemblage that includes hornblende and biotite.

All amphiboles analyzed from the core zone gneisses are retrograde including those from eclogites. In general, amphiboles yielded high apparent $^{40}Ar/^{39}Ar$ ages in the first ~5 to 10% of the gas released. This is interpreted to be the result of incorporation of excess argon (Figure 3a). Amphibole from sample 89301 gave high apparent ages in the first ~6% of the gas released followed by a gradient from 1.8 to ~3.0 Ma. The last 10% of the gas released gave progressively younger apparent ages from ~3.0 to ~2.4 Ma. The best estimate of the age of amphibole from sample 89303 is 2.71 Ma based on 73% of the gas released. The $^{40}Ar/^{39}Ar$ apparent ages range from 2.0 to 3.1 Ma and 1.9 to 3.0 Ma for amphibole from samples 89304 and 89308, respectively. In summary, age spectra for amphiboles from the core zone show high apparent ages in the first few percent of the gas released followed by ages that rise from ~1.8 to 2.4 Ma. However, the bulk of the amphibole spectra for core zone gneisses indicate $^{40}Ar/^{39}Ar$ apparent ages of 2.4 to 2.7 Ma.

Biotites from core zone gneisses yielded relatively flat age spectra with $^{40}Ar/^{39}Ar$ apparent ages that range, in general, from 1.5 to 1.7 Ma (Figure 3b). The data plotted on an isochron diagram (Figure 3c) indicates the trapped argon for all biotites has an atmospheric composition ($^{40}Ar/^{36}Ar = 295.5$) and indicates a combined age of 1.64 ± 0.03 Ma.

Plagioclase from felsic core zone gneisses yielded saddle-shaped spectra interpreted to be the result of incorporation of varying degrees of excess Ar (Figure 3d). Plagioclase minimum apparent ages of 4.2 and 2.3 Ma (for samples 89301 and 89303, respectively) are interpreted to be the maximum age(s) for cooling below the closure temperature for plagioclase. Sample inhomogeneity is evident for 89301 as the integrated $^{40}Ar/^{39}Ar$ age (12.96 ± 0.48 Ma) is not concordant with the total fusion age of 9.25 ± 0.44 Ma. Results for both plagioclase samples when plotted on an inverse isochron diagram cluster close to the y axis and show a high degree of scatter.

Fission track results. Apatites from the core zone gneisses indicate fission track ages that range from 0.3 to 0.9 Ma (Table 3). Errors associated with these analyses overlap and a mean age for the five samples analyzed is 0.7 ± 0.2 Ma. Ages of 0.4 and 0.5 Ma for samples 89303 and 89305 are the most precise analyses for core zone gneisses due to the relatively high U concentration, large size, and high quality of their apatite grains. The large error associated with eclogite sample 89313 is a reflection of the low U concentration of the apatites.

Shear Zone Rocks

$^{40}Ar/^{39}Ar$ and K/Ar results. $^{40}Ar/^{39}Ar$ analyses on muscovites from gneisses associated with several different shear zones are shown on a composite age spectra in Figure 4a. The Morima shear zone muscovites yielded significantly older $^{40}Ar/^{39}Ar$ apparent ages than results from other shear zone gneisses. In general, $^{40}Ar/^{39}Ar$ apparent ages for muscovites from the Morima shear zone range between 3.6 and 4.0 Ma. In contrast, muscovites from the Wakonai shear zone and

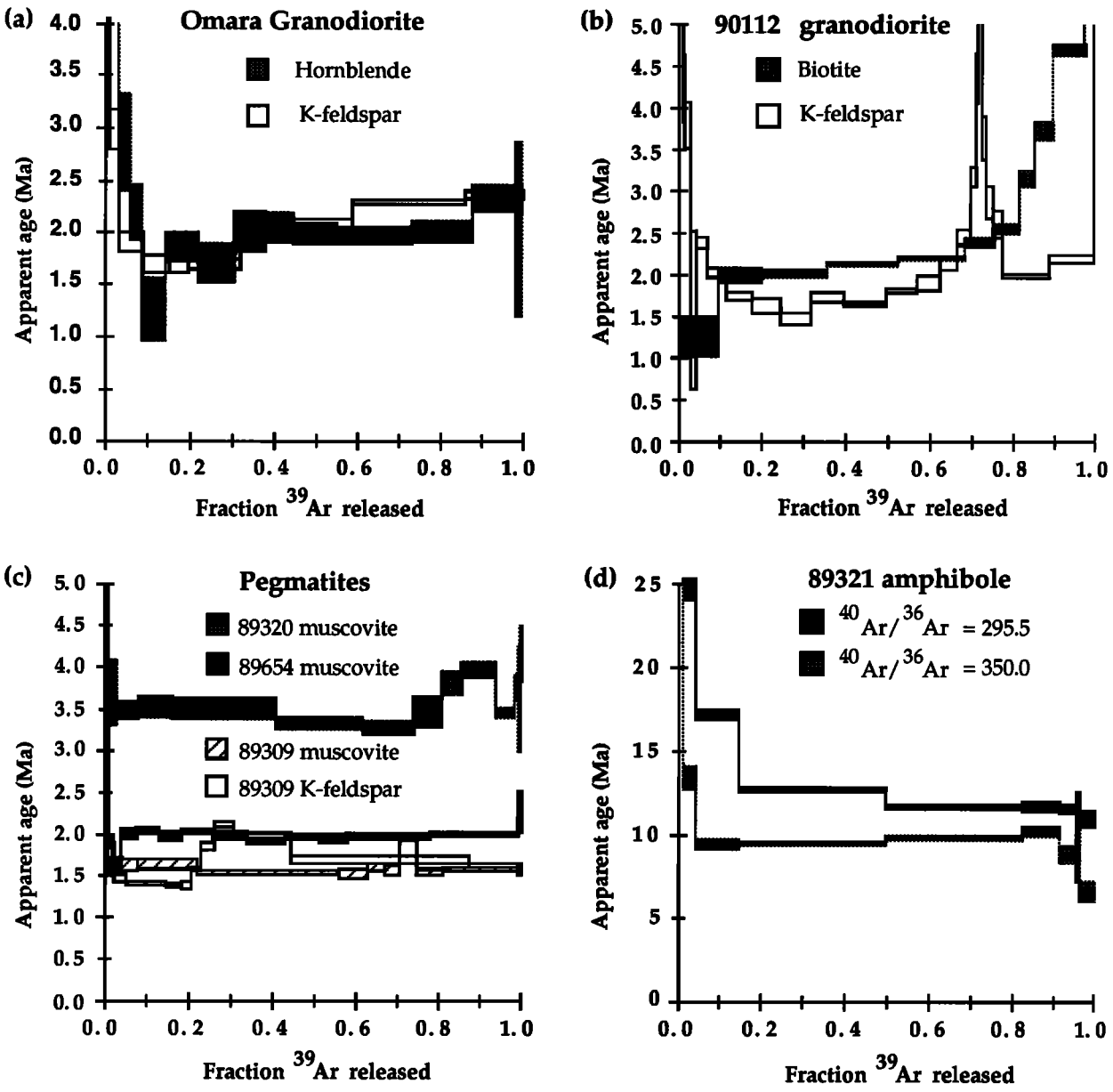

Fig. 5. $^{40}Ar/^{39}Ar$ age spectra for (a) hornblende and K-feldspar from the Omara granodiorite; (b) biotite and K-feldspar from undeformed granodiorite which intrudes ultramafic rocks at Mebulibuli; (c) muscovite and K-feldspars from pegmatites from the D'Entrecasteaux Islands; (d) amphibole from a retrograde eclogite xenolith in granodiorite from Tumabaguna Island.

the Wadelai shear zone yielded $^{40}Ar/^{39}Ar$ apparent ages of ~1.6 to 1.8 Ma.

Age spectra for biotites from Wakonai and Mwadeia shear zones are shown in Figure 4b. In general, $^{40}Ar/^{39}Ar$ apparent ages range from 1 to 2 Ma. However, the high temperature portion of the age spectrum for sample 90115, corresponding to the last 10% of the gas released, yielded $^{40}Ar/^{39}Ar$ apparent ages which rise sharply from 2.0 Ma to ~4.5 Ma.

Potassium feldspars from shear zone gneisses yielded age spectra that are characterized by low $^{40}Ar/^{39}Ar$ apparent ages ranging from approximately 1.2 to 1.9 Ma and corresponding to 50 to 60% of the gas released. These segments of the age spectra are relatively flat (Figure 4c). The last ~40% of the gas released for shear zone feldspars gave progressively older $^{40}Ar/^{39}Ar$ apparent ages. In general, sample 89650 yielded the youngest $^{40}Ar/^{39}Ar$ apparent ages ranging from 1.0 to 2.0 Ma. Sample 89323 yielded the oldest $^{40}Ar/^{39}Ar$ apparent ages for K-feldspars from shear zone gneisses; these ranged from ~1.9 to 2.2 Ma.

Fission track results. Fission track analyses on apatites from the shear zone gneisses gave ages that ranged from 0.4 to 1.0 Ma, with a mean age of 0.8 ± 0.2 Ma (Table 3). The

TABLE 3. Apatite Fission Track Dating Results for Samples from the D'Entrecasteaux Islands

Sample	Number of Crystals	$\rho_S(N_S)$,[a] x 10^5 cm^{-2}	$\rho_i(N_i)$,[b] x 10^6 cm^{-2}	(ρ_S/ρ_i)[c]	$P(\chi^2)$,[d] %	r[e]	$\rho_D(N_D)$,[f] x 10^6 cm^{-2}	U, ppm	Fission Track Age, Ma ± 1σ
89-301	30	0.0222 (5)	0.585 (1317)	0.004 ± 0.002	79.1	0.196	1.229 (2768)	6.2	0.8 ± 0.4
89-303	20	0.0145 (2)	0.861 (1187)	0.002 ± 0.001	65.8	0.208	1.229 (2768)	9.8	0.4 ± 0.3
89-305	20	0.0484 (7)	1.891 (2734)	0.003 ± 0.003	27.1	0.348	1.229 (2768)	20.2	0.5 ± 0.2
89-307	20	0.0235 (4)	0.590 (1005)	0.004 ± 0.002	23.8	0.100	1.229 (2768)	6.3	0.9 ± 0.4
89-313	22	0.0183 (2)	0.425 (463)	0.002 ± 0.001	99.8	0.737	1.229 (2768)	2.8	0.9 ± 0.7
89-316	20	0.0297 (5)	0.828 (1394)	0.003 ± 0.001	92.2	0.449	1.229 (2768)	8.8	0.8 ± 0.3
89-317	20	0.0793 (10)	2.402 (3029)	0.004 ± 0.001	77.5	0.543	1.229 (2768)	25.6	0.7 ± 0.2
89-318	20	0.1057 (10)	2.925 (2767)	0.004 ± 0.001	96.0	0.478	1.229 (2768)	31.2	0.8 ± 0.3
89-319	10	0.0666 (6)	2.762 (2488)	0.002 ± 0.001	33.5	0.029	1.427 (3215)	25.4	0.6 ± 0.2
89-323	17	0.0315 (4)	0.851 (1097)	0.002 ± 0.001	21.6	0.246	1.427 (3215)	7.8	0.9 ± 0.5
89-325	20	0.0528 (9)	1.164 (1985)	0.004 ± 0.001	97.7	0.529	1.229 (2768)	12.1	1.0 ± 0.2
89-327	20	0.0089 (1)	0.325 (361)	0.003 ± 0.003	44.6	0.022	1.427 (3215)	3.0	0.7 ± 0.7
89-329	20	0.0362 (5)	0.631 (872)	0.004 ± 0.002	94.4	0.504	1.229 (2768)	6.7	1.2 ± 0.6
89-331	20	0.0167 (3)	1.097 (1976)	0.002 ± 0.001	30.2	0.114	1.427 (3215)	10.1	0.4 ± 0.2
89-650	11	0.0483 (3)	1.052 (654)	0.006 ± 0.004	36.1	0.351	1.229 (2768)	11.2	1.0 ± 0.6
89-654	20	0.0271 (3)	0.828 (918)	0.003 ± 0.002	93.1	0.391	1.427 (3215)	7.6	0.8 ± 0.5
population age of all samples		0.0382 (79)	1.083 (24247)						0.8 ± 0.1

Apatite ages calculated using a zeta of 353 for NBS glass SRM 612 [Green, 1985].

[a] ρ_S-spontaneous track density: N_S number of spontaneous tracks counted.

[b] ρ_i-induced track density: N_i-number of induced tracks counted.

[c] $(\rho_S/\rho_i$ -mean of individual crystal ratios (± 1σ) for those analyses giving $P(\chi^2)$ <5%.

[d] $P(\chi^2)$ probability of obtaining observed χ^2 value for v degrees of freedom (v = number of crystals-1).

[e] r-correlation coefficient between individual crystal track counts (N_S and N_i).

[f] ρ_D track density measured in external detector adjacent to the glass dosimeter during irradiation. N_D number of tracks counted in determining ρ_D.

TABLE 4. Summary of Thermochronologic Data for Samples from the D'Entrecasteaux Islands, PNG

Sample	Lithology	Thermochronology[a]	Comments
		Core Zone[b]	
89301	felsic gneiss	3.00 Ma (hbl)[c], 1.56 Ma (bio; 3.1)*, 4.17 Ma (plag)[d], 9.40 Ma (K/Ar;plag), 0.8 Ma(ft;ap)	excess Ar in plag; hbl and bio retrograde
89303	felsic gneiss	2.71 Ma (hbl)[e], 1.61 Ma (bio; 2.5)*, 2.29 Ma (plag)[d], 0.4 (ft;ap)	plag excess Ar; hbl plateau; hbl and bio retrograde
89304	eclogite	2.67 Ma (hbl; 6.9)*	hbl retrograde
89305	felsic gneiss	0.5 Ma (ft;ap)	
89307	int-mafic gneiss	1.67 Ma (bio; 2.0)*; 0.9 Ma(ft;ap)	bio retrograde
89313	eclogite	0.9 Ma (ft;ap)	
		Shear Zones	
89316	gneiss	0.8 Ma (ft;ap)	Wakonai extensional shear zone
89317	felsic gneiss	0.7 Ma (ft;ap)	Wakonai extensional shear zone
89318	schist	1.53 Ma (wm; 4.2)*; 1.41 Ma (bio)[c]; 1.42 Ma (kspar)[c];0.8 Ma (ft;ap)	Wakonai extensional shear zone
89323	quartzo-feldspathic schist	2.03 Ma (kspar)[c]; 2.00 Ma (K/Ar; kspar); 0.9 Ma (ft;ap)	Normanby shear zone
89330	felsic gneiss	3.91 Ma (wm)[c]	Morima shear zone
89331	felsic gneiss	3.67 Ma (wm)[c]; 1.88 Ma (kspar)[c]; 1.93 Ma (K/Ar;kspar); 0.4 Ma (ft;ap)	Morima shear zone
89650	felsic gneiss	1.49 Ma (wm)[c]; 1.11 Ma (kspar; 3.7)*; 1.0 Ma (ft;ap);	Wadelai transverse shear zone
90115	sheared felsic gneiss	1.90 Ma (bio)[c]	Mwadeia extensional shear zone
		Intrustives	
89308	eclogite xenolith	2.67 Ma (hbl; 10.4)*; 1.71 Ma (bio; 12.5)*	hbl and bio retrograde; Galuwata
89309	granodiorite	1.82 Ma (kspar)[c]; 1.9 Ma (K/Ar;kspar); 1.55 Ma (wm; 2.2)*	~2% excess Ar in kspar; Galuwata
89319	granodiorite	0.6 Ma (ft;ap)	Tumabaguna Island
89320	pegmatite	3.52 Ma (wm)[c]	Tumabaguna Island
89321	eclogite xenolith	9.83 Ma(amph; 12.3)*	amph retrograde, excess Ar in amph; Tumabaguna Island
89324	dolerite dike	1.8 Ma (K/Ar;wr)	crosscuts granodiorite; Normanby Island
89325	granodiorite	2.0 Ma (K/Ar;kspar); 1.0 Ma(ft;ap)	Normanby Island
89327	foliated granodiorite	1.91 Ma (kspar)[c];1.9 Ma (K/Ar;kspar); 0.7 Ma (ft;ap)	Guletabutabu
89329	granodiorite	1.8 Ma (K/Ar;kspar); 1.2 Ma (ft;ap)	Normanby Island
89652	granodiorite	2.17 Ma (kspar)[c]; 2.29 Ma Ma(hbl)[c]	hbl, kspar contain excess Ar in low temperature steps, Omara granodiorite
89654	deformed pegmatite	1.99 Ma (wm)[c]; 0.8 Ma (ft;ap);	Morima shear zone
90112	granodiorite	1.81 Ma (kspar; 21.1)*; 2.07 Ma (bio; 49.5)*	undeformed and intrudes ultramafic rocks; Mebulibuli
		Upper Plate	
89322	andesite	0.8 Ma (K/Ar;wr)	

Material analyzed indicated in parentheses. Abbreviations for minerals are hornblende (hbl), apatite (ap), white mica (wm), biotite (bio), plagioclase (plag) and K-feldspar (kspar); whole rock (wr).

[a]All ages are $^{40}Ar/^{39}Ar$ apparent ages except where otherwise indicated; apatite fission track (ft;ap) ages indicate cooling to ≤130°C; K/Ar apparent ages (K/Ar).

[b]All core zone samples from Galuwata River transect into Goodenough dome.

[c]Integrated $^{40}Ar/^{39}Ar$ age; see text for discussion of closure temperatures.

[d]Lowest apparent age on saddle-shaped spectrum.

[e]Plateau age.

*Isochron age with MSWD indicated in parentheses.

apatite samples from the shear zones were generally of very high quality. Most apatites were large and had relatively high U concentrations (one grain contained >30 ppm U). The consistent quality of these samples resulted in relatively precise apatite fission track ages despite the fact the samples are ≤1 Ma.

Intrusives

Granodiorites: $^{40}Ar/^{39}Ar$ and K/Ar results. Granodiorites which intrude the basement gneisses contain the assemblage plagioclase (zoned oligoclase-andesine) + K-feldspar + quartz + calcic-amphibole + biotite + opaques + sphene. Hornblende from the Omara granodiorite shows high $^{40}Ar/^{39}Ar$ apparent ages associated with the first 8% of the gas released interpreted to be the result of excess Ar (Figure 5a). A plateau age of 2.0 Ma is indicated for ~60% of the gas released. Potassium feldspar from the Omara granodiorite also shows high apparent ages corresponding to the first 9% of the gas released. The remainder of the age spectrum is characterized by apparent ages that progressively rise from 1.7 to 2.4 Ma. Sample 90112 is from an undeformed granodiorite that intrudes ultramafic rocks of the upper plate. The biotite spectrum yielded $^{40}Ar/^{39}Ar$ apparent ages that progressively rise from 1.3 Ma to 2.4 Ma for 80% of the gas released. The final 20% of the gas released yielded significantly higher $^{40}Ar/^{39}Ar$ apparent ages of 2.6 to 4.7 Ma (Figure 5b) which corresponds with relatively high $^{37}Ar/^{39}Ar$ ratios. These results are similar to those obtained for a biotite from the Mwadeia shear zone (90115) and may be the result of the degassing of a high Ca/K phase (amphibole or pyroxene intergrowths/inclusions?) at high temperatures.

K/Ar ages for feldspars from four granodiorite samples range from 1.8 to 2.0 Ma (Table 1). A step heat experiment of sample 89327 K-feldspar yielded a relatively flat age spectrum corresponding to $^{40}Ar/^{39}Ar$ apparent ages of 1.8 to 2.0 Ma (Table 1).

Granodiorites: Fission track results. Apatite fission track ages from four granodiorite samples (89319, 89325, 89327, and 89329) range from 0.6 to 1.2 Ma and give a mean age of 0.9 ± 0.2 Ma. The ages for samples 89329 and 89327 have low precision because they had relatively low U concentrations.

Pegmatites: $^{40}Ar/^{39}Ar$ and K/Ar results. Pegmatites which intrude the basement gneisses, and shear zones are associated with granodiorites. They contain quartz + K-feldspar + muscovite. Muscovite from sample 89320 yielded $^{40}Ar/^{39}Ar$ apparent ages that range in general from 3.3 Ma to 4.0 Ma. In contrast muscovites from samples 89654 and 89309 yielded relatively flat spectra corresponding to $^{40}Ar/^{39}Ar$ apparent ages of 2.0 Ma and 1.6 Ma. Potassium feldspar (89309) yielded a complex pattern with $^{40}Ar/^{39}Ar$ apparent ages ranging from 1.4 to 2.0 Ma.

Pegmatites: Fission track results. Sample 89654 yielded an apatite fission track age of 0.8 ± 0.5 Ma.

Xenoliths: $^{40}Ar/^{39}Ar$ and K/Ar results. Granodiorite which intrudes the basement contains xenoliths of retrograded eclogite. Reaction rinds of amphibole surround the eclogite xenoliths and this in turn is often surrounded by pegmatitic material. Results of step heating experiments on amphibole from an eclogite rind are shown in Figure 5d. The amphibole gave a complex pattern with ages progressively decreasing from greater than 90 Ma to 10 Ma with increasing temperature during the step heat experiment. An isochron plot for this sample suggests an age of 11.0 ± 0.6 Ma and a trapped initial argon composition of ~350 (mean square of weighted deviates (MSWD) = 12). Significantly lower $^{40}Ar/^{39}Ar$ apparent ages are obtained if the $^{40}Ar/^{36}Ar$ ratio indicated from the isochron plot is used to reduce the data; these results are shown in Figure 5d and indicate ages of 9.0 to 10.4 Ma corresponding to ~80% of the gas released. The K/Ca ratios corresponding to each temperature step vary considerably for this sample and may reflect degassing of different phases. The $^{40}Ar/^{39}Ar$ apparent ages for hornblende and biotite (89308) from the rind of another xenolith in granodiorite from Goodenough Island gave apparent ages of ~2.7 and 1.7 Ma, respectively.

Dolerite dike. A dolerite dike which crosscuts granodiorite on Normanby Island gave a whole rock K-Ar age of 1.8 Ma.

Upper Plate Rocks

K/Ar results indicate an age of 0.78 Ma for an andesite ash flow tuff from Fergusson Island.

DISCUSSION

Interpretation of Thermochronologic Data and Closure Temperatures

Information concerning the thermal history of samples can be inferred from the form of $^{40}Ar/^{39}Ar$ age spectra (see McDougall and Harrison [1988] for a review). Samples that remain stable during vacuum heating and exhibit flat age spectra are often interpreted as indicating that the mineral has remained thermally undisturbed since crystallization and cooled rapidly. In these samples radiogenic argon is believed to be distributed uniformly within crystals. Hydrous phases which are unstable in the vacuum furnace (e.g., argon is released by a mechanism involving a phase change [Gaber et al., 1988]) and exhibit flat age spectra may also contain uniformly distributed radiogenic argon within the crystals. Alternatively, flat spectra in these samples may result from homogenization of discrete gas reservoirs during vacuum heating. It is interesting to note that sample 89650 yielded flat age spectra for both K-feldspar (believed to be stable in the vacuum furnace to temperatures below approximately 1150°C), as well as muscovite, and biotite. In general, most of the hornblendes, biotites, muscovites, and some of the K-feldspars analyzed in this study yielded relatively flat age spectra. Our interpretation of these spectra is that the samples have cooled rapidly and have remained thermally undisturbed since cooling below their respective closure temperatures.

The near concordancy of apparent ages for minerals with different closure temperatures provides additional evidence that these samples cooled rapidly. For example, hornblende and K-feldspar from the Omara granodiorite (89652) gave concordant $^{40}Ar/^{39}Ar$ apparent ages for approximately 60% of the gas

released (Figure 5a). These data indicate the sample cooled at rates that were >>100°C/m.y., and spent very little time in the transition from open to closed system behavior for argon in hornblende and K-feldspar. Similarly muscovite, biotite, and K-feldspar from the Wakonai shear zone (89318) also yielded relatively flat age spectra with nearly concordant $^{40}Ar/^{39}Ar$ isochron ages of 1.53 Ma, 1.45 Ma and 1.24 Ma, respectively.

In contrast, samples which have cooled slowly and/or experienced partial argon loss due to a thermal event will likely exhibit spectra with age gradients. A limited amount of evidence exists for partial reheating due to a thermal event in some of the age spectra. For example, several hornblende spectra from core zone gneisses show age gradients in the low temperature portion of the age spectra which resemble theoretical age spectra [Turner, 1968] for ~20% argon loss due to a thermal event at ≤2 Ma.

If metamorphism occurs well above the closure temperatures for argon retention, as in the case of the D'Entrecasteaux Island metamorphic rocks, $^{40}Ar/^{39}Ar$ analyses of amphiboles, muscovite, biotite and feldspars will provide ages corresponding to the time at which the samples cooled to below their respective closure temperatures. Closure temperatures for these minerals

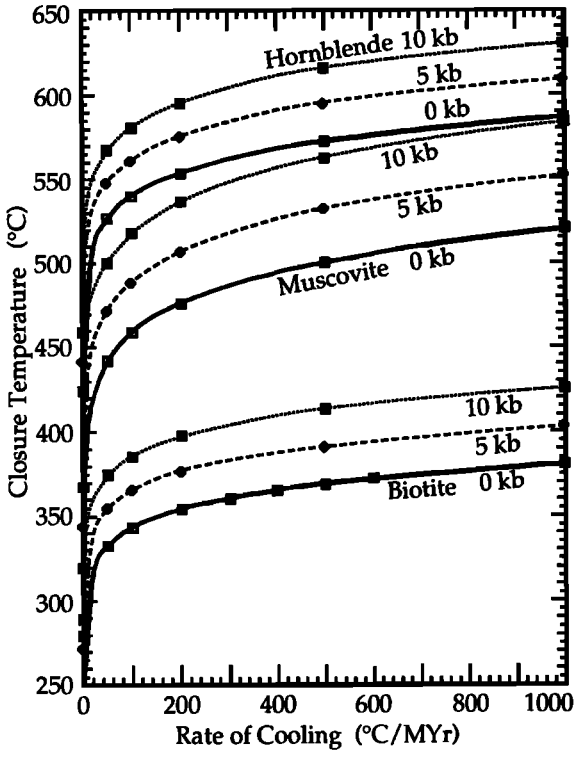

Fig. 6. Plot of closure temperature versus cooling rate for hornblende, muscovite, and biotite. Curves for mean stress of 0 kbar, 5 kbar, and 10 kbar indicated. The following diffusion parameters were used in the calculations: (1) hornblende: spherical geometry, E = 64.1 kcal/mol, D_0 = 0.024 cm^2/s [Harrison, 1981], V = 14 cm^3/mol [Harrison et al., 1985], a = 70 μm; (2) muscovite: slab geometry, E = 40 kcal/mol, D_0 = 6.03 x 10^{-7} cm^2/s [Robbins, 1972], V = 14 cm^3/mol [Harrison et al., 1985], a = 70 μm; (3) biotite: infinite cylinder model, An_{56}, E = 47.0 kcal/mol, D_0 = 0.77 cm^2/s, V = 14 cm^3/mol, a = 150 μm [Harrison et al., 1985].

are often quoted in the literature as having values of ~500°C [Harrison, 1981; Baldwin et al., 1991], ~350°C [Robbins, 1972], ~300°C [Harrison et al., 1985], and ~350° to 150°C [Lovera et al., 1989], respectively, for moderate cooling rates. Closure temperatures increase with an increase in cooling rate [Harrison, 1981] and higher mean stress [Harrison et al., 1985]. Figure 6 illustrates the relationship between cooling rate, closure temperature, and mean stress for hornblende, muscovite, and biotite assuming a single activation energy and a single diffusion domain (see figure caption for choice of parameters used in the calculations). Results of thermochronologic studies of the basement gneisses, shear zone rocks, and intrusives from the D'Entrecasteaux Islands indicate rapid cooling of the metamorphic core complex from approximately 4.0 Ma to 0.5 Ma. The rocks of the lower plate cooled at rates as high as 200° to 400°C/m.y., so that closure temperatures for hornblende, muscovite, and biotite are likely to have been significantly higher (i.e., approximately 550° to 570°C, 480° to 500°C, and 350° to 360°C, respectively). An additional increase in closure temperature results from the effects of mean stress at the time of closure. For example, if the mean stress at time of closure is 10 kbar for hornblende, 8 kbar for muscovite, and 5 kbar for biotite, closure temperatures would be elevated further to approximately 590° to 610°C, 520° to 540°C, and 375° to 385°C, respectively.

T-t History of the Lower Plate

In general, for a given sample hornblende records the oldest $^{40}Ar/^{39}Ar$ apparent ages. Muscovite, biotite, and K-feldspar record progressively younger $^{40}Ar/^{39}Ar$ apparent ages. Apatite fission track ages record the youngest ages and normally indicate when the sample cooled to ~<100°C, but for such high cooling rates, the closure temperature would be closer to 130°C. Plagioclases gave anomalously high $^{40}Ar/^{39}Ar$ apparent ages interpreted to be due to incorporation of excess argon. Hornblende, muscovite, biotite, and K-feldspar which formed at midcrustal levels in the D'Entrecasteaux region, have trapped argon compositions which appear to be close to atmospheric (e.g., Figure 3c). A temperature-time history for the core zone gneisses, shear zone gneisses, and intrusives based on $^{40}Ar/^{39}Ar$ and fission track results is shown in Figure 7.

Amphibole samples from basement gneisses, granodiorites and reaction rinds around xenoliths gave apparent ages in general that range from 1.8 to 2.8 Ma. Muscovites, from pegmatites, and shear zone gneisses yielded two groups of ages, 3.5 to 4.0 and ~1.5 to 2.0 Ma. Biotites gave apparent ages of between ~1.4 and 1.9 Ma.

Core zone gneisses cooled rapidly at rates of ~100° to 200°C/m.y. (Figure 7). Shear zones were active at several different times (see discussion below), but in general, ages range from 1.5 to 2.0 and 3.5 to 4.0 Ma. The older Morima shear zone cooled relatively slowly (~80° to 120°C/m.y.) compared with the Wadelai shear zone (~480°C/m.y.) and Wakonai shear zone (~625°C/m.y.) which both cooled extremely fast. T-t data for intrusive rocks also indicated high, variable cooling rates. Granodiorite (89320 and 89319) from Tumabaguna Island cooled relatively slowly compared to the Omara granodiorite which cooled rapidly (>500°C/m.y.) as indicated by concordant hornblende and K-feldspar $^{40}Ar/^{39}Ar$ ages and zircon $^{206}Pb^*/^{238}U$ ages [Baldwin et al., 1992].

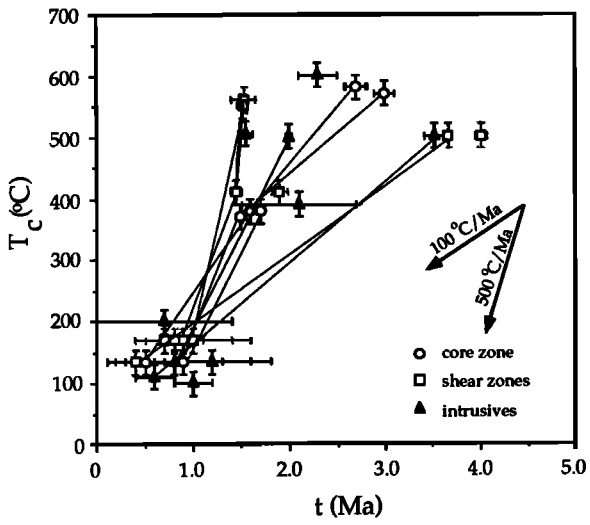

Fig. 7. Temperature-time curves for samples from the D'Entrecasteaux Islands.

The extremely rapid cooling of the lower plate rocks and shear zone rocks was not solely due to loss of heat by conduction. In fact, if anything, the heat flux at the base of the crust likely increased during core complex formation as a result of upwelling mantle related to the Woodlark Basin spreading center. The ~50 km of tectonic unroofing necessary to explain the presence of eclogites at the surface today was accomplished largely by movement on faults and shear zones bounding the D'Entrecasteaux core complexes [Hill et al., 1992] and resulted in extremely rapid cooling of the metamorphic basement, shear zone rocks, and intrusions.

Intrusions

Approximately 30 to 40% of the basement rocks in the D'Entrecasteaux Islands consist of undeformed and deformed granodiorite. Structural relationships indicate two phases of granodiorite emplacement; the early phase occurred before or during early stages of shear zone activity, and the second phase occurred during the late stages of shear zone activity [Hill, 1991]. Emplacement of the plutons postdates all preshear zone deformation and there is a clear relationship both spatially and chronologically between extensive granodiorite plutonism, shear zone deformation and the exhumation of the high-grade metamorphic rocks which comprise the basement. Bouguer anomalies around the D'Entrecasteaux Islands confirm that there is a broad spatial correlation between the high-grade metamorphic rocks and the intrusion of large granodiorite bodies. At least two major episodes of granodiorite intrusion can be delineated on the basis of structural and geochronological relationships. Older intrusives and sheared equivalents(?) (~3.5 to 4.0 Ma; Table 4) were emplaced prior to, or at the onset of shearing and contain pervasively developed mylonitic shear zone fabrics [Hill et al., 1992]. These ages may represent an earlier phase of cooling following intrusion of the older plutons. Subsequent widespread resetting of argon systematics was likely the result of high temperatures which prevailed during the second phase of intrusive activity. Resetting of argon systematics was heterogeneous due to very localized and transient effects of contact metamorphism. Younger plutons (~1.5 to 2.0 Ma), which are largely undeformed except for local cross-cutting shear zones, were emplaced late during shearing. Mapping of the Omara Pluton indicates the pluton may be sheetlike; the upper boundary is approximately horizontal and is strongly discordant to compositional layering and macroscopic structures [Hill et al., 1992]. The late stages of deformation and uplift of rocks in the D'Entrecasteaux Islands are synchronous not only with plutonism but also with extensive volcanism [Smith, 1976; Smith and Compston, 1982] based on concordant ages. Rapid uplift of the basement rocks also likely triggered relatively minor amounts of decompression melting in the basement rocks as indicated by the presence of several phases of migmatization, as well as small granitic veins and pegmatites [Hill, 1991]. However, structural and geochronologic evidence indicates that shear zone movement and uplift of the basement occurred as a result of intrusion.

Shear Zones

Two major sets of shear zones have been recognized in the D'Entrecasteaux Islands [Hill, 1991]. The first set of shear zones are northeasterly dipping shear zones which bound the northeastern sides of the domes and indicate a normal or oblique-normal sense of shear. They form the boundary between the high-grade metamorphic basement and the relatively undeformed mafic and ultramafic rocks of the upper plate and are interpreted to represent a major extensional detachment surface. Normal movement along the detachment surface likely provided a mechanism for the uplift and tectonic exhumation of the metamorphic basement [Hill et al., 1992]. Shear zones that are transverse to the main detachment (i.e., bound the eastern and western sides of the domes) have oblique or horizontal stretching lineations and are overlain by basement rocks as well as ultramafic cover rocks.

The transverse zones and extensional domes appear to be interconnected; the detachment is offset in a sinistral direction where it is intersected by the transverse zones. $^{40}Ar/^{39}Ar$ results indicate the extensional (Wakonai and Mwadeia; Figure 2) and transverse (Wadelai) shear zones record similar cooling histories. The age spectra for muscovites and K-feldspars from the Wakonai shear zone and the Wadelai shear zone are nearly identical (Figures 4a and 4c; Table 4) suggesting they may have been operative at the same time and experienced similar thermal histories. Biotites from extensional shear zones yielded similar $^{40}Ar/^{39}Ar$ ages although, in general, biotite ages from the Mwadeia shear zone are slightly older (1.5 to 2.0 Ma) than those from the Wakonai shear zone (1.0 to 1.7 Ma).

Overall the $^{40}Ar/^{39}Ar$ apparent ages obtained for the two sets of shear zones (i.e., extensional and transverse), the metamorphic grade of the mylonitic foliation, and the structural continuity of the shear zones [Hill, 1991] suggests that both sets of shear zones operated contemporaneously. Movement along the shear zones had likely ceased by approximately 1.4 Ma because the closure temperatures are lower than what are indicated by the metamorphic assemblages preserved.

The Morima shear zone is enigmatic; it is located on the southern side of Fergusson Island, dips southwards, and microstructures indicate a consistent sinistral sense of motion [Hill, 1991]. $^{40}Ar/^{39}Ar$ results on muscovites and K-feldspars indicate this shear zone underwent a significantly different thermal history. The muscovites record significantly older $^{40}Ar/^{39}Ar$ apparent ages (3.7 and 4.0 Ma). K-feldspar (89331)

from the Morima shear zone, in general, yielded $^{40}Ar/^{39}Ar$ apparent ages which were significantly older (1.5 to 2.4 Ma) than K-feldspars from the extensional shear zones (1.2 to 1.5 Ma for Wakonai; 1.0 to 1.5 Ma for Wadelai).

We propose that the Morima shear zone cooled rapidly through the transition zone for argon retention in muscovite (to temperatures << 540° to 520°C) from 4.0 to 3.7 Ma. These samples were apparently not affected by later shearing/intrusive events at 1 to 2 Ma. K-feldspars from the Morima shear zone either record a subsequently more protracted cooling history from 2.4 to 1.5 Ma or were partially reset by subsequent thermal events. If the later scenario holds true, then high temperatures were not sustained long enough to reset the muscovites (i.e., the thermal event was short-lived and not intense).

P-T-t History of the Lower Plate and Shear Zones

Figure 8 illustrates the P-T-t history of the lower plate and shear zones. Thermobarometry was used to obtain P-T constraints for peak metamorphism in the core zone gneisses, retrogression in the shear zone rocks and retrogression in the core zone gneisses [Hill and Baldwin, 1993]. Eclogites record peak metamorphic conditions of 18 to 21 kbar and 730° to 900°C. Temperatures in the basement during eclogite formation were too high for argon to be retained in any of the minerals analyzed, therefore none of the $^{40}Ar/^{39}Ar$ apparent ages records this event. The oldest $^{40}Ar/^{39}Ar$ apparent age

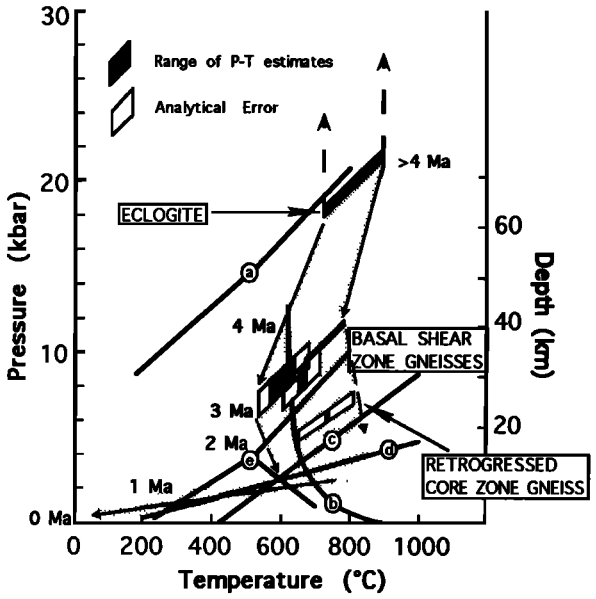

Fig. 8. P-T-t path for the D'Entrecasteaux metamorphic core complexes. Ages are based on $^{40}Ar/^{39}Ar$ apparent ages and fission track ages. Thermobarometry from Hill and Baldwin [1993]. Path is constrained by (1) mafic eclogites from core zone, (2) shear zone gneisses, (3) re-equilibrated core zone gneiss. Reaction lines are shown for (a) jadeite + quartz = albite [Gasparik and Lindsley, 1980]; (b) granite minimum melt curve; (c) almandine + kyanite = hercynite + quartz [Holland and Powell, 1990]; (d) pyrope + kyanite = spinel + plagioclase [Holland and Powell, 1990]; (e) Al_2SiO_5 polymorphs [Holdaway, 1971].

(9.8 Ma) was measured on retrograde hornblende from an eclogite xenolith in granodiorite on Tumabaguna Island; we are uncertain as to where the xenolith originated. Since this age is anomalous and the majority of the analyses are less than 4.0 Ma, we feel the best estimate for the timing of eclogite facies metamorphism is constrained to be greater than 4.0 Ma. White micas from the Morima shear zone and white mica from a pegmatite on Tumabaguna Island record cooling at 3.5 to 4.0 Ma. This suggests that an earlier phase of intrusion and movement on the Morima shear zone commenced prior to 4.0 Ma. Subsequently, the metamorphic basement experienced rapid decompression from 4.0 Ma to 2.0 Ma.

Deformation and amphibolite facies metamorphism formed basal shear zone gneisses at depths of approximately 25 to 35 km prior to 2 Ma. Temperatures and pressures apparently decreased during shear zone formation as indicated by lower pressures (7 to 9 kbar) and slightly lower temperatures (570° to 670°C) and by zoning in garnets consistent with decreasing temperatures [Hill and Baldwin, 1993].

During the final stages of exhumation the Omara granodiorite was emplaced at 2.1 to 2.2 Ma at pressures of 4 to 5 kbar [Hill and Baldwin, 1993]. The core zone gneisses reequilibrated at relatively low pressures (~5 to 6 kbar), but high temperatures (~730°C). These high temperatures were likely due to intrusion of late stage granodiorites and resulted in localized contact metamorphism and retrogression of the metamorphic basement. Late stage development of hercynite and sillimanite in some of the gneisses lends further support for high temperatures at relatively low pressures [Hill and Baldwin, 1992]. Thermal gradients within the core zone and shear zones were heterogeneous and resulted in widespread resetting of argon systematics. However, maximum temperatures were not high enough and the duration of the thermal event was not long enough to reset the Morima shear zone samples and those from Tumabaguna Island. The subsequent P-T-t path involved extremely rapid cooling (~400°C/m.y.) of basement gneisses, intrusions, and shear zone gneisses from 2.0 to 1.0 Ma. Apatite fission track ages record the final stages of cooling between 0.4 and 1.2 Ma. In summary, unroofing rates on the order of 10 mm/yr over periods of ~4 m.y. are required to explain the P-T-t path followed by the D'Entrecasteaux rocks.

Role of Magmatism in the Formation of the Metamorphic Core Complexes

A summary of Neogene-Quaternary events in the D'Entrecasteaux region is shown in Figure 9. The main rifting phase in the Woodlark Basin began ~3.5 Ma and opened 16° [Weissel et al., 1982]. The $^{40}Ar/^{39}Ar$ results presented here indicate that retrogression/cooling of the basement was coincident with cooling of the granodiorites. Shear zone minerals such as muscovite also gave similar ages. From ~4 Ma to 1.5 Ma stretching of the crust, exhumation, and intrusion appear to have occurred virtually simultaneously in this region. Volcanism may have begun in the region in early Pliocene time and has continued to the present. Uplift of the domes above sea level is correlated with the early to mid-Pliocene terrestrial sedimentation in the Cape Vogel Basin [Tjhin, 1976] to the northeast of the D'Entrecasteaux Islands.

Thermochronologic results of the D'Entrecasteaux metamorphic core complexes confirm that magmatism is of first-order significance in the extension process. In this region the conti-

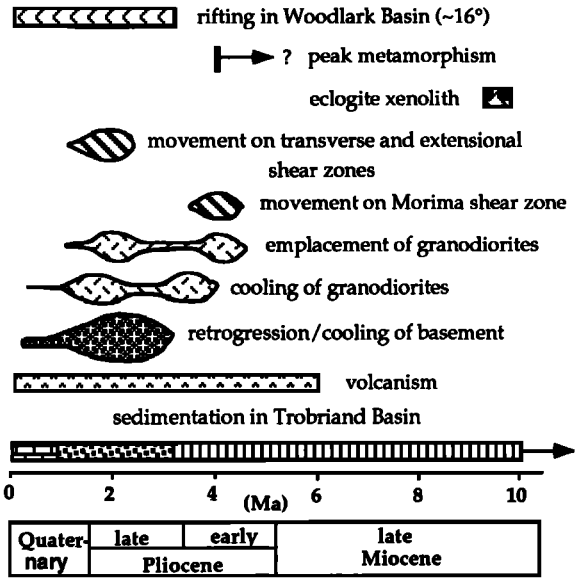

Fig. 9. Neogene-Quaternary events in the D'Entrecasteaux region (modified from Davies and Warren [1988]). Patterns for sediments in the Trobraind Basin are as follows: limestone (brick), shale and conglomerate (solid circles), and shale (vertical lines).

nental crust was thickened as the result of previous compressional orogeny, and the availability of magma may have been determined by the propagation of a spreading center into continental crust. It has been previously noted that a clear spatial and temporal link exists between metamorphic core complex formation and plutonic activity [see Crittenden et al., 1980, and references therein] and that magma may play an important role in the mechanics of continental extension [Lachenbruch and Morgan, 1990]. However, in many core complexes evidence for plutonism synchronous with mylonitization is lacking. The synchroneity of magma emplacement with deformation in kilometer thick ductile shear zones in the domes of the D'Entrecasteaux Islands has been demonstrated by thermochronologic results presented here. In this region uplift of the metamorphic basement and widespread plutonism are closely correlated.

The D'Entrecasteaux metamorphic core complexes may provide a modern analogue for metamorphic core complexes which have formed throughout Earth's history. In the Solomon Sea, an active spreading center is propagating into previously thickened continental crust. Thermochronologic results indicate that exhumation and cooling of the basement was coincident with westward propagation of the spreading center. Thickened continental crust is being torn apart, due to interaction with the Woodlark Basin spreading center with the consequence that very high pressure metamorphic rocks have been brought to the surface in the past 4 million years without having been completely retrogressed. This exceedingly rapid uplift seems to be an intrinsic part of the pattern that is emerging from many of the extensional terrains [cf., Zeck et al., 1992], where metamorphic rocks are uplifted and exposed at the surface as the result of extensional orogeny.

The domal form of the core complexes and their present high elevations (up to 2.5 km above sea level) lead us to argue for the fundamental involvement of magmatism in their formation. It is proposed that heating of thickened continental crust beneath the D'Entrecasteaux Islands due to mantle upwelling triggered melting which produced granodiorite magmas (Figure 10). The thickened continental crust weakens as the result of this magmatic activity, and continental extension begins, with the formation of crustal scale shear zones. Ongoing magmatism then leads to the continual intrusion of magma, at crustal levels determined by lithospheric strength as well as by the geochemistry of the magma. Continued extension of the crust results in extremely rapid uplift of the basement rocks. Granitoid magma continually arrives and crystallizes, liberating large volumes of fluid. Retrograde assemblages in the core zone rocks are largely hydrous phases (amphibole, micas) indicating that addition of fluids during retrograde metamorphism may have occurred. The addition of fluids would also result in lowering the temperature of melting in the basement rocks. Some intrusions may have been emplaced at shallow levels of the crust and cooled rapidly while others may have been emplaced at great depths, uplifted rapidly and subsequently cooled. Crustal scale ductile shear zones begin to form in the roof zone as movement zones localize. Tectonic denudation caused rapid uplift of high pressure metamorphic rocks and resulted in rapid cooling of the core complex. Continued uplift is accentuated by the continual arrival of magma at depth and results in the presently observed topography. Granodiorite emplacement caused local heating and resulted in the formation of local topographic highs (i.e., the D'Entrecasteaux domes).

What remains unclear is whether the spreading center is seeking out the weakest zone (in this case, thickened continental crust) to propagate. Although at 2 to 3 Ma the surface expression of the oceanic spreading center is along strike and east of the region of intra-"continental" extension, we believe that upwelling of mantle material is providing significant heat input to the base of thickened continental crust in the D'Entrecasteaux region. At present the rift is propagating into continental lithosphere and the resulting overall geometry mimics oceanic propagation [Mutter et al., 1992]. Extension postdates compression in this young orogenic belt.

CONCLUSIONS

Thermochronologic results for the D'Entrecasteaux Islands' metamorphic basement, granodiorites, and shear zone rocks indicate very rapid cooling of this young orogenic belt. Formation and unroofing of the domes occurred in Plio-Pleistocene time and is directly related to the propagation of the Woodlark Basin spreading center westward into the continental margin of PNG. Magmatism is of first-order significance in the extension process and in the formation of the D'Entrecasteaux metamorphic core complexes. In the D'Entrecasteaux region the continental crust was thickened as a result of previous compressional orogeny and the heat which was critical to the production of magmas was provided by upwelling mantle associated with the propagation of a spreading center into continental crust. The D'Entrecasteaux core complexes represent a modern analogue for metamorphic core complexes which form as a result of interaction with a spreading center.

Uplift and retrogression of the metamorphic basement are closely correlated with widespread plutonism. Metamorphic basement and granodiorites cooled rapidly (>>100°C/m.y.) from ~3.0 to 1.5 Ma. During this time the D'Entrecasteaux

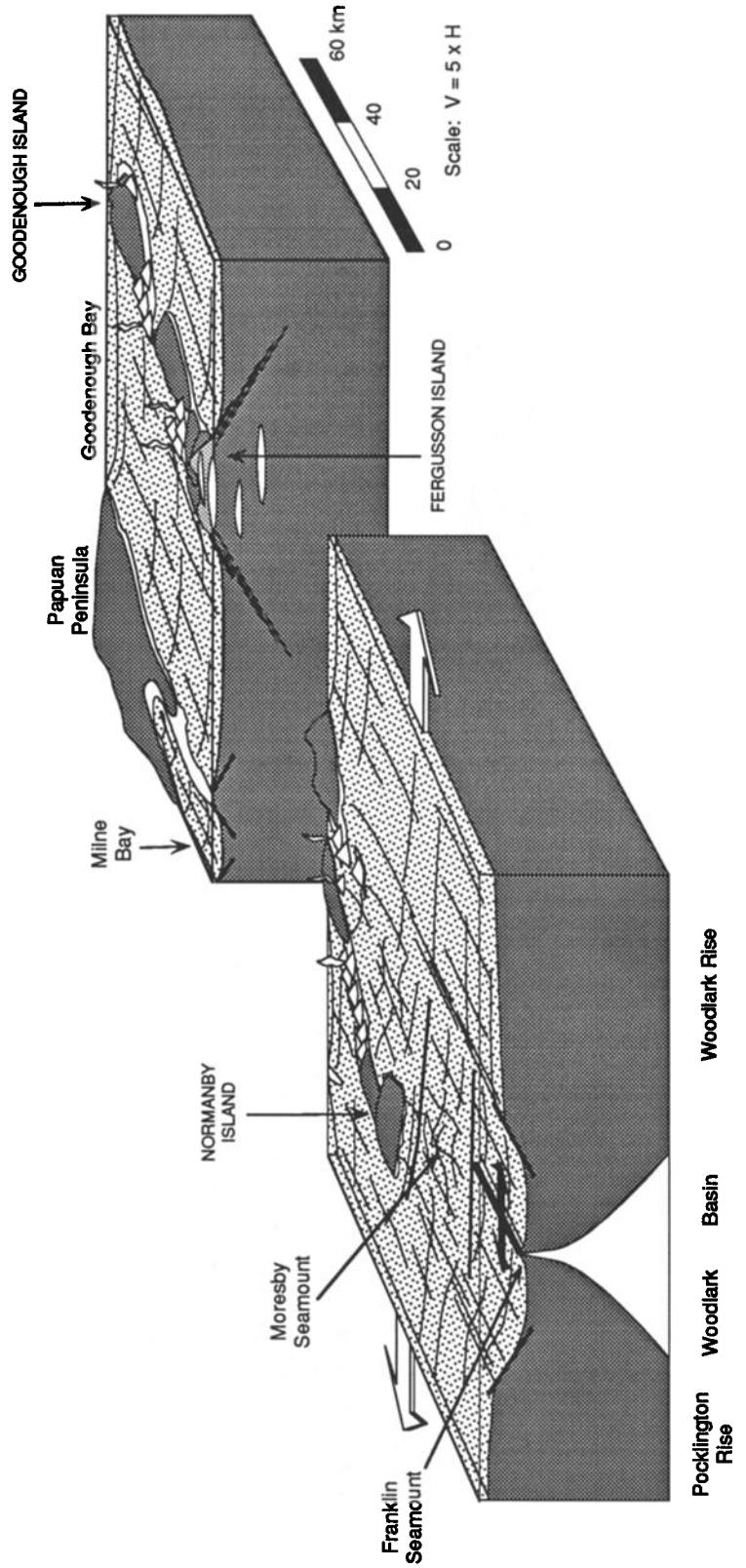

Fig. 10. Schematic block diagram of the D'Entrecasteaux Islands and west Woodlark Basin showing major structural features. The D'Entrecasteaux Islands are aligned with the axis of seafloor spreading and rifting in the Woodlark Basin. Grabens are bounded by approximately east-west trending normal faults and offset in places by sinistral transfer faults (e.g., Moresby transfer fault (MTF) and Normanby Transfer Fault (NTF). There is a close temporal and spatial association between unroofing of deep crustal rocks in the D'Entrecasteaux Islands and extensive plutonism and volcanism.

region is believed to have undergone approximate north-south directed extension as the result of interaction with the Woodlark Basin spreading center.

Acknowledgments. S. L. Baldwin , E. J. Hill, and G. S. Lister gratefully acknowledge City Resources P.N.G. Inc. and INCO (Canada) for logistical support during field work. This study is part of an Australian Research Council grant "Continental Extension Tectonics" awarded to G. S. Lister, A. J. W. Gleadow, and G. Houseman. Support for irradiations was provided by the Australian Institute of Nuclear Science and Engineering and the Australian Nuclear Science and Technology Organization. We thank J. Mya, R. Maier, R. Rudowski, H. Kokkonen, and R. Van De Vusse for technical support, and J. Delhaize and J. Overs for assistance in preparation of the manuscript. Paul Fitzgerald, Jon Spencer, and Steve Richard provided helpful discussion, and comments. Reviews by John Mutter and Peter Zeitler are gratefully acknowledged. We especially thank the people of the D'Entrecasteaux Islands for their help during our field work without which this project would not have been possible, in particular David Peniasi of Fergusson Island.

REFERENCES

Abers, G., Possible seismogenic shallow-dipping normal faults in the Woodlark-D'Entrecasteaux extensional province, Papua New Guinea, *Geology, 19*, 1205-1208, 1991.

Audley-Charles, M. G., Tectonics of the New Guinea area, *Annu. Rev. Earth Planet. Sci., 19*, 17-41, 1991.

Baldwin, S. L., T. M. Harrison, and J. D. Fitz Gerald, The diffusion of ^{40}Ar in metamorphic hornblende, *Contrib. Mineral. Petrol., 105*, 691-703, 1991.

Baldwin, S. L., T. R. Ireland, and R. Rudowski, 2.8 Ga zircons in Plio-Pleistocene sediments from the Trobriand Basin, Solomon Sea, *Eos Trans. AGU, 73*, 573, 1992.

Binns, R. A., S. D. Scott, R. V. Burne, R. L. Chase, D. R. Cousens, A. W. S. Denton, R. J. Edwards, E. J. Finlayson, M. P. Gorton,T. F. McConachy, A. W. Poole, and D. J. Whitford, Ridge propagation into continental crust: the April 1986 PACLARK cruise to western Woodlark Basin (abstract), *Eos Trans. AGU, 67*, 1231, 1986.

Bryant, B., C. W. Naeser, J. E. Fryxell, Implications of low-temperature cooling history on a transect across the Colorado Plateau-Basin and Range Boundary, west central Arizona, *J. Geophys. Res., 96*, 12375-12388, 1991.

Carl, B. S., C. F. Miller, D. A. Foster, Western Old Woman Mountains shear zone: Evidence for latest Cretaceous core complex development in southeastern California?, *Geology, 19*, 893-896, 1991.

Cooper, P., and B. Taylor, Seismotectonics of New Guinea: A model for arc reversal following arc-continent collision, *Tectonics, 6*, 53-67, 1987.

Crittenden, M. D., P. J. Coney, and G. H. Davis, editors, Cordilleran metamorphic core complexes, *Mem. Geol. Soc. Am. 153*, 490 pp.,1980.

Curtis, J. W., The spatial seismicity of Papua New Guinea and the Solomon Islands, *J. Geol. Soc. Aust., 20*, 1-20, 1973.

Davies, H. L., Fergusson Island, Papua New Guinea, scale 1:250,000 geological series explanatory notes, 25 pp., Dept. of Miner. and Energy, Bur. of Miner. Resour., Canberra, Australia, 1973.

Davies, H. L., and D. J. Ives, The geology of Fergusson and Goodenough Islands, Papua, *Rep. Bur. Miner. Resour. Geol. Geophys. Aust., 65*, 1-83, 1965.

Davies, H. L., and A. L. Jacques, Emplacement of ophiolite in Papua New Guinea, *Spec. Publ. Geol. Soc London, 13*, 341-350, 1984.

Davies, H. L., and I. E. Smith, Geology of Eastern Papua, *Geol Soc. Am. Bull., 82*, 3299-3312, 1971.

Davies, H. L., and R. G. Warren, Origin of eclogite-bearing, domed, layered metamorphic complexes ("core complexes") in the D'Entrecasteaux Islands, Papua New Guinea, *Tectonics, 7*, 1-21, 1988.

Davies, H. L., and R. G. Warren, Eclogites of the D'Entrecasteaux Islands, *Contrib. Mineral. Petrol.*, in press, 1993.

Davies, H. L., P. A. Symonds, and I. D. Ripper, Structure and evolution of the southern Solomon Sea region, *BMR J. Aust. Geol. Geophys., 9*, 49-68, 1984.

Davis, G. A., G. S. Lister, and S. J. Reynolds, Structural evolution of the Whipple and South Mountain shear zones, southwestern United States, *Geology, 14*, 7-10, 1986.

DeWitt, E., J. F. Sutter, G. A. Davis, and J. L. Anderson, $^{40}Ar/^{39}Ar$ age spectrum dating of Miocene mylonitic rocks, Whipple Mountains, southeastern California, *Geol. Soc. Am. Abstr. Programs, 18*, 584, 1986.

Dokka, R. K., and S. H. Lingrey, Fission track evidence for a Miocene cooling event, Whipple Mountains, southeastern California, in *Cenozoic Paleogeography of the Western United States*, edited by J. Armentrout, M. Cole, and H. Terbest, pp. 141-145, Pacific Section, Society of Economic Paleontologists and Mineralogists, Bakersfield, Calif., 1979.

Dokka, R. K., M. J. Mahaffie, and A. W. Snoke, Thermochronologic evidence of major tectonic denudation associated with detachment faulting, northern Ruby Mountains-east Humboldt range, Nevada, *Tectonics, 5*, 995-1006, 1986.

Foster, D. A., T. M. Harrison, C. F. Miller, and K. A. Howard, The $^{40}Ar/^{39}Ar$ thermochronology of the eastern Mojave Desert, California, and adjacent western Arizona with implications for the evolution of metamorphic core complexes, *J. Geophys. Res., 95*, 20000-20024, 1990.

Gaber, J. G., K. A. Foland, and C. E. Corbato, On the significance of argon release from biotite and amphibole during $^{40}Ar/^{39}Ar$ vacuum heating, *Geochim. Cosmochim. Acta, 52*, 2457-2465, 1988.

Gans, P. B., An open-system, two layer crustal stretching model for the Eastern Great Basin, *Tectonics, 6*, 1-12, 1987.

Gans, P. B., E. L. Miller, R. Brown, G. Houseman, and G. S. Lister, Assessing the amount, rate, and timing of tilting in normal fault blocks: a case study of tilted granites in the Kern-Deep Creek Mountains, Utah, *Geol. Soc. Am. Abstr. Programs, Cordilleran Section, 23*, 28, 1991.

Gasparik, T. and D. H. Lindsley, Phase equilibria at high pressures of pyroxenes containing monovalent and trivalent ions, in *Pyroxenes, Reviews in Mineralogy*, vol. 7, edited by C. T. Prewitt, pp. 309-340, Mineralogical Society of America, 1980.

Gibson, G. M., Uplift and exhumation of middle and lower crustal rocks in an extensional tectonic setting, Fiordland, New Zealand, in *Exposed Cross-Sections of the Continental Crust*, edited by M. H. Salisbury and D. M. Fountain, pp. 71-101, Kluwer Academic, Hingham, Mass., 1990.

Green, P. F., A new look at statistics in fission track dating, *Nucl. Tracks, 5*, 77-86, 1981.

Green, P. F., Comparison of zeta calibration baselines for fission track dating of apatite, zircon, and sphene, *Isot. Geosci., 58*, 1-22, 1985.

Green, P. F., On the thermo-tectonic evolution of northern England: Evidence from fission track analyses, *Geol. Mag., 123*, 493-506, 1986.

Harrison, T. M., Diffusion of ^{40}Ar in hornblende, *Contrib. Mineral. Petrol., 78*, 324-331, 1981.

Harrison, T. M., I. Duncan, and I. McDougall, Diffusion of ^{40}Ar in biotite: Temperature, pressure and compositional effects, *Geochim. Cosmochim. Acta, 49*, 2461-2468, 1985.

Hill, E. J., Active extension in the D'Entrecasteaux Islands, Papua New Guinea, in *Bureau of Mineral Resources Research Symposium 87 (Extended Abstracts)*, pp. 51-57, Australian Government Publishing Service, Canberra, Australia, 1987.

Hill, E. J., The nature of shear zones formed during extension in eastern Papua New Guinea, paper presented at Pacific Rim Congress, Gold Coast, Australia , 1990.

Hill, E. J., Metamorphic core complexes in the D'Entrecasteaux Islands, Papua New Guinea, Ph.D. thesis, Monash Univ., Melbourne, Australia, 1991.

Hill, E. J., and S. L. Baldwin, Exhumation of high pressure metamorphic rocks during crustal extension in the D'Entrecasteaux region, Papua New Guinea, *J. Metamorph. Geol., 11*, 261-277, 1993.

Hill, E. J., S. L. Baldwin, and G. S. Lister, Unroofing of active metamorphic core complexes in the D'Entrecasteaux Islands, Papua New Guinea, *Geology, 20*, 907-910, 1992.

Holdaway, M. J., Stability of andalusite and the aluminum silicate phase diagram, *Am. J. Sci., 271*, 97-131, 1971.

Holland, T. J. B., and R. Powell, An enlarged and updated internally consistent thermodynamic dataset with uncertainties and correlations: The system K_2O-Na_2O-CaO-MgO-MnO-FeO-Fe_2O_3-Al_2O_3-TiO_2-SiO_2-C-H_2-O_2, *J. Metamorph. Geol., 8*, 89-124, 1990.

Hurford, A. J., and P. F. Green, A users guide to fission track dating calibration, *Earth Planet. Sci. Lett., 59*, 343-354, 1982.

Johnson, R. W., D. E. MacKenzie, and I. E. M. Smith, Volcanic rock associations at convergent plate boundaries: reappraisal of the concept using case histories from Papua New Guinea, *Geol. Soc. Am. Bull., 89*, 96-106, 1978.

Johnson, T., and P. Molnar, Focal mechanisms and plate tectonics of the southwest Pacific, *J. Geophys. Res.*, *77*, 5000-5032, 1972.

Lachenbruch, A. H., and P. Morgan, Continental extension, magmatism, and elevation; formal relations and rules of thumb, *Tectonophysics*, *174*, 39-62, 1990.

Lister, G. S., and G. A. Davis, Models for the formation of metamorphic core complexes and mylonitic detachment terranes, *J. Struct. Geol.*, *11*, 65-94, 1989.

Lister, G. S., G. Banga, and A. Feenstra, Metamorphic core complexes of Cordilleran type in the Cyclades, Aegean Sea, Greece, *Geology*, *12*, 221-225, 1984.

Lovera, O. M., F. M. Richter, and T. M. Harrison, The $^{40}Ar/^{39}Ar$ thermochronology for slowly cooled samples having a distribution of domain sizes, *J. Geophys. Res.*, *94*, 17917-17931, 1989.

Luyendyk, B. P., K. C. MacDonald, and W. B. Bryan, Rifting history of the Woodlark Basin in the southwest Pacific, *Geol. Soc. Am. Bull.*, *84*, 1125-1134, 1973.

McDougall, I., K-Ar and $^{40}Ar/^{39}Ar$ dating of hominid-bearing Pliocene-Pleistocene sequence at Koobi Fora, Lake Turkana, northern Kenya, *Geol. Soc. Am. Bull.*, *96*, 159-175, 1985.

McDougall, I. and T. M. Harrison, *Geochronology and thermochronology by the $^{40}Ar/^{39}Ar$ method*, 212 pp., Oxford University Press, New York, 1988.

McDougall, I., and Z. Roksandic, Total fusion $^{40}Ar/^{39}Ar$ ages using HIFAR reactor, *J. Geol. Soc. Aust.*, *21*, 81-89, 1974.

Miller, E. L., P. B. Gans, and J. D. Garing, The Snake Range decollement: An exhumed mid-Tertiary ductile-brittle transition, *Tectonics*, *2*, 239-263, 1983.

Milsom, J., The gravity field of the Papuan Peninsula, *Geol. Mijnbouw*, *52*, 13-20, 1973.

Milsom, J., and I.E. Smith, Southeastern Papua: Generation of thick crust in a tensional environment?, *Geology*, *3*, 117-120, 1975.

Mutter, J. C., J. B Diebold, C. Z. Mutter, G. Abers, S Scott, V. Benes, G. Lister, and A. K. Pahl, Continental breakup by rift propagation in the Woodlark Basin/D'Entrecasteaux Islands mimics oceanic propagation, *Eos Trans. AGU*, *73*, 536, 1992.

Norman, M. D., and S. L. Baldwin, Geochemistry of high-grade metamorphic rocks and granodiorites, D'Entrecasteaux Islands, Papua New Guinea, pp. 82-83, annual report, Res.Sch. Earth Sci., The Aust. Nat. Univ., Canberra, 1990.

Ollier, C. D., and C. F. Pain, Actively rising surficial gneiss domes in Papua New Guinea, *J. Geol. Soc. Aust.*, *27*, 33-44, 1980.

Rehrig, W. A., Processes of regional Tertiary extension in the western Cordillera: Insights from the metamorphic core complexes, Spec. Pap. *Geol. Soc. Am.*, *208*, 97-121, 1986.

Richard, S. M., J. F. Fryxell, and J. F. Sutter, Tertiary structure and thermal history of the Harquahalla and Buckskin mountains, west central Arizona: Implications for denudation by a major detachment fault system, *J. Geophys. Res*, *95*, 19973-19987, 1990.

Ripper, I. D., Seismicity of the Indo-Australian/Solomon Sea plate boundary in the southeast Papua region, *Tectonophysics*, *87*, 355-369, 1982.

Robbins, G. A., Radiogenic argon diffusion in muscovite under hydrothermal conditions, M.Sc. thesis, 189 pp., Brown Univ., Providence, R.I., 1972

Smith, I. E. M., Peralkaline rhyolites from the D'Entrecasteaux Islands, Papua New Guinea, in *Volcanism in Australasia*, edited by R. W. Johnson, pp. 275-285, Elsevier, New York, 1976.

Smith, I. E. M., and W. Compston, Strontium isotopes in Cenozoic volcanic rocks from southeastern Papua New Guinea, *Lithos*, *15*, 199-206, 1982.

Smith, I. E. M., and J.S. Milsom, Late Cenozoic volcanism and extension in eastern Papua, in Marginal Basin Geology, edited by M. Kokelaar and K. Howells, *Geol. Soc. London*, *16*, 163-171, 1984.

Steiger, R. H., and E. Jäger, Subcommission on geochronology: convention on the use of decay constants in geo- and cosmochronology, *Earth Planet. Sci. Lett.*, *36*, 359-362, 1977.

Stolz, A., S. C. McCluskey, P. J. Morgan, and K. Lambeck, Comparison of 1981 satellite Doppler and 1990 GPS baseline measurements across a plate boundary complex in Papua New Guinea (abstract), *Eos Trans. AGU*, *71*, 1272, 1990.

Tetley, N., I. McDougall, and H. R. Heydegger, Thermal neutron interferences in the $^{40}Ar/^{39}Ar$ dating technique, *J. Geophys. Res.*, *85*, 7201-7205, 1980.

Tjhin, K. T., Trobriand Basin Exploration, *APEA J.*, *16*, 81-90, 1976.

Turner, G., The distribution of potassium and argon in chondrites, in *Origin and Distribution of the Elements*, edited by L. H. Ahrens, pp. 387-398, Pergamon, New York, 1968.

Weissel, J. K., B. Taylor, and G. D. Karner, The opening of the Woodlark Basin, subduction of the Woodlark spreading system and the evolution of northern Melanesia since mid-Pliocene time, *Tectonophysics*, *87*, 253-277, 1982.

Wernicke, B., Low angle normal faults in the Basin and Range province: Nappe tectonics in an extending orogen, *Nature*, *291*, 645-648, 1981.

Wernicke, B., Uniform-sense normal simple shear of the continental lithosphere, *Can. J. Earth Sci.*, *22*, 108-125, 1985.

Worthing, M. A., Petrology and tectonic setting of blueschist facies metabasites from the Emo Metamorphics of Papua New Guinea, *Aust. J. Earth Sci.*, *35*, 159-168, 1988.

Zeck, H. P., P. Monie, I. M. Villa, and B. T. Hansen, Very high rates of cooling and uplift in the Alpine belt of the Betic Cordilleras, southern Spain, *Geology*, *20*, 79-82, 1992.

S. L. Baldwin, Department of Geosciences, University of Arizona, Tucson, AZ 85721.

D. A. Foster, V.I.E.P.S. Department of Geology, La Trobe University, Bundoora, Victoria 3083, Australia.

E. J. Hill, Department of Geology, University of Otago, Dunedin, New Zealand.

G. S. Lister, V.I.E.P.S. Department of Earth Sciences, Monash University, Clayton, Victoria 3168, Australia.

I. McDougall, Research School of Earth Sciences, Australian National University, Canberra, Australian Capital Territory 2601, Australia.

(Received June 17, 1992;
revised January 19, 1993;
accepted January 26, 1993.)